

St. John's University

**St. John's Scholar**

---

Theses and Dissertations

---

2022

**REPURPOSING OF SMALL MOLECULE INHIBITOR YM-155  
INHIBITS HIGH-RISK NEUROBLASTOMA GROWTH BY DIRECTLY  
INHIBITING SURVIVIN PROTEIN**

Danielle Crystal Rouse

Follow this and additional works at: [https://scholar.stjohns.edu/theses\\_dissertations](https://scholar.stjohns.edu/theses_dissertations)



Part of the [Pharmacy and Pharmaceutical Sciences Commons](#)

---

**REPURPOSING OF SMALL MOLECULE INHIBITOR YM-155  
INHIBITS HIGH-RISK NEUROBLASTOMA GROWTH BY  
DIRECTLY INHIBITING SURVIVIN PROTEIN**

A thesis submitted in partial fulfillment  
of the requirements for the degree of

**MASTER OF SCIENCE**

to the faculty of the

DEPARTMENT OF PHARMACEUTICAL SCIENCES

of

COLLEGE OF PHARMACY AND HEALTH SCIENCES

at

ST. JOHN'S UNIVERSITY

New York

by

**DANIELLE C. ROUSE**

Date Submitted \_\_\_\_\_

Date Approved \_\_\_\_\_

\_\_\_\_\_  
Danielle Rouse

\_\_\_\_\_  
Dr. Saurabh Agarwal

**© Copyright by Danielle C. Rouse 2022**

**All Rights Reserved**

## **ABSTRACT**

### **REPURPOSING OF SMALL MOLECULE INHIBITOR YM-155 INHIBITS HIGH-RISK NEUROBLASTOMA GROWTH BY DIRECTLY INHIBITING SURVIVIN PROTEIN**

**DANIELLE C. ROUSE**

High-risk neuroblastoma (NB) is an aggressive pediatric tumor which develops from the extracranial sympathetic nervous system and accounts for almost 15% of all childhood cancer-related deaths. Current therapies include high-dose chemotherapy and radiation which have long-term toxic side-effects. Despite these intensive therapies, the overall survival rate of NB is less than 50%. Therefore, developing novel therapeutic approaches by directly targeting the molecular mechanisms that drives NB progression is very important. In the present study, we analyzed genomic datasets of 1235 NB patients and discovered that overexpression of survivin coding gene BIRC5 strongly correlates with poor overall and event-free survival of NB patients, and more aggressive tumors have significantly higher BIRC5 levels. Survivin belongs to the inhibitor of apoptosis protein family and is known to be involved in controlling cell division and apoptosis. Oncogenic activation of survivin has been reported in different cancers including NB. To further understand the role of survivin in NB, we repurposed a survivin inhibitor YM-155. Cell viability assays in six NB cell lines demonstrated the potency of YM-155 in significantly inhibiting NB cell proliferation. Additionally, clonogenic and 3D-spheroid formation assay results showed that YM-155 significantly inhibits colony formation and 3D-spheroid size respectively. Furthermore, apoptosis and cell cycle assays in different NB cell lines in response to increasing concentration of YM-155 revealed significantly higher apoptosis and blockage of cell cycle progression in comparison to control treatments. Molecular

assays including gene expression profiling and Western blotting further confirmed that YM-155 directly inhibits survivin at both mRNA and protein levels in NB. To further develop an effective therapeutic approach, we combined YM-155 with the chemotherapy drug etoposide. This dual therapy combination revealed that YM-155 synergistically sensitizes NB to chemotherapy treatment. Overall, our pre-clinical data demonstrates that repurposing YM-155 and combining it with current therapies is a novel, less-toxic, and more-effective therapeutic approach for NB.

## ACKNOWLEDGEMENTS

Words cannot fully express my appreciation and gratitude to my mentor Dr. Saurabh Agarwal, whose immense and constant support, encouragement, and trust have propelled me to complete my Master research work! I am inspired and thankful for the wealth of scientific knowledge, and wisdom he has imparted as a credible researcher. He has further bolstered my personal and professional growth by sharing invaluable lessons throughout my Masters' journey.

Sincere thanks to my committee members Dr. Sunil Kumar, and Dr. Vikas Dukhande for agreeing to serve, and lend their scientific expertise, in reading and evaluating this thesis. Their guidance in my coursework and research provision is noteworthy.

I would like to thank the Department of Pharmaceutical Sciences at St. John's University for their academic and financial support, and Chair Dr. Vijaya Korlipara, for her administrative help throughout my graduate studies. It would be remiss of me not to extend heartfelt thanks to Dr. Marc Gillespie, now Vice Provost, who has been a tremendous source of support and guidance as I navigated this degree. To my lab-mates Rameswari Chilamakuri, Bharti Sharma, and Jawaher Alkhamisy, thank you for your advice and suggestions as I developed my research. I also want to extend thanks to all the undergraduate students in Dr. Agarwal's lab, whom I had the opportunity to work with, learn from, and teach. Additionally, thanks to the Science Supply team for your meaningful support.

They say, "it takes a village", and I am thankful for mine! To my beloved parents- Samuel & Darena Rouse, sisters- Piea-Marrie Crichlow & Riea Rouse, niece- Kim-Marrie

Crichlow, granny- Ceciline, aunt- Carol, uncles- Dr. Edward, Ronald & Victor, extended family, church family, pray warriors, colleagues, and friends too numerous to mention them all- Anjali, Clint, Disney Gang Gang family, Jamal, Kelsha, Kerisha, Kevin, Kia, Kristen, Lamar, Nethania, Oluwaseyi, Rafael, Shari, Shonnella, and Tové, thank you. Your prayers, encouragement, love and accountability as I “mastered” this degree has been prodigiously comforting spiritually, mentally and emotionally. We did it!

For I know the plans I have for you, “declares the Lord,” plans to prosper you and not to harm you, plans to give you hope and a future. (Jeremiah 29:11) The Greatest Of All Time (G.O.A.T)- God, avowed this, not just for me, but also for you, and I am forever grateful for His plan being fulfilled in my life.

## TABLE OF CONTENTS

<b>ACKNOWLEDGEMENTS .....</b>	<b>ii</b>
<b>LIST OF TABLES .....</b>	<b>vi</b>
<b>LIST OF FIGURES .....</b>	<b>vii</b>
<b>CHAPTER 1 .....</b>	<b>1</b>
<b>1. INTRODUCTION .....</b>	<b>1</b>
1.1 NEUROBLASTOMA.....	1
1.2 p53.....	2
1.3 SURVIVIN (BIRC5) .....	4
1.4 YM-155.....	8
<b>CHAPTER 2 .....</b>	<b>9</b>
<b>2. MATERIALS &amp; METHODS .....</b>	<b>9</b>
2.1 CHEMICALS & REAGENTS .....	9
2.2 CLINICAL PATIENT DATASETS.....	11
2.3 CELL CULTURE & MAINTENANCE.....	11
2.4 PREPARATION OF DRUG TREATMENT SOLUTIONS .....	12
2.5 CELL VIABILITY USING MTT ASSAY.....	13
2.6 CLONOGENIC ASSAY .....	14
2.7 3D-SPHEROID ASSAY.....	14
2.8 APOPTOSIS ASSAY .....	16

2.9 CELL CYCLE ASSAY .....	16
2.10 RNA EXTRACTION, cDNA SYNTHESIS and QUANTITATIVE RT-PCR	18
2.11 IMMUNOBLOTTING ASSAYS .....	20
2.12 SYNERGY STUDIES .....	21
2.13 STATISTICAL ANALYSIS .....	21
<b>CHAPTER 3.....</b>	<b>22</b>
<b>3. RESULTS .....</b>	<b>22</b>
3.1 BIRC5 EXPRESSION CORRELATES WITH POOR NB PROGNOSIS .....	22
3.2 YM-155 INHIBITS NB PROLIFERATION .....	26
3.3 YM-155 INDUCES APOPTOSIS AND BLOCKS CELL CYCLE .....	31
3.4 YM-155 INHIBITS NB SPHEROID GROWTH.....	34
3.5 YM-155 INHIBITS SURVIVIN PATHWAY TO SUPPRESS NB GROWTH	43
3.6 YM-155 SENSITIZES NB TO CHEMOTHERAPY .....	46
<b>CHAPTER 4.....</b>	<b>55</b>
<b>4. DISCUSSION .....</b>	<b>55</b>
<b>REFERENCES.....</b>	<b>58</b>

## LIST OF TABLES

<b>Table 1.</b> Primers used to perform gene expression experiments.....	10
--	----

## LIST OF FIGURES

<b>Figure 1.</b>	The role of p53 during tumor progression.....	3
<b>Figure 2.</b>	Survivin Structure.....	5
<b>Figure 3.</b>	Control of survivin expression at the mRNA and protein level.....	7
<b>Figure 4.</b>	BIRC5 expression correlates with poor overall survival of NB patients...	23
<b>Figure 5.</b>	BIRC5 expression correlates with NB progression.....	24
<b>Figure 6.</b>	BIRC5 expression correlates with MYCN Amplified cells and NB progression.....	25
<b>Figure 7.</b>	YM-155 inhibits NB proliferation in MYCN Non-amplified cell lines....	27
<b>Figure 8.</b>	YM-155 inhibits NB proliferation in MYCN Amplified cell lines.....	28
<b>Figure 9.</b>	YM-155 inhibits NB colony formation in MYCN Non-amplified cell lines.....	29
<b>Figure 10.</b>	YM-155 inhibits NB colony formation in MYCN Amplified cell lines...	30
<b>Figure 11.</b>	YM-155 induces apoptosis in NB cells.....	32
<b>Figure 12.</b>	YM-155 blocks cell cycle progression in NB cells.....	33
<b>Figure 13.</b>	YM-155 inhibits NB spheroid tumor growth in SH-SY5Y cells.....	35
<b>Figure 14.</b>	YM-155 inhibits NB spheroid tumor growth in IMR-32 cells.....	37
<b>Figure 15.</b>	YM-155 inhibits NB 3D-spheroid tumor growth in SH-SY5Y cells.....	39
<b>Figure 16.</b>	YM-155 inhibits NB 3D-spheroid tumor growth in IMR-32 cells.....	41
<b>Figure 17.</b>	YM-155 inhibits Survivin pathway at mRNA level.....	44

<b>Figure 18.</b> YM-155 inhibits Survivin pathway at protein level.....	45
<b>Figure 19.</b> YM-155 enhances VP-16 induced cytotoxicity in MYCN Non- amplified NB cell lines.....	47
<b>Figure 20.</b> YM-155 enhances VP-16 induced cytotoxicity in MYCN Amplified NB cell lines.....	49
<b>Figure 21.</b> YM-155 sensitizes NB MYCN Non-amplified cell lines to chemotherapy VP-16.....	51
<b>Figure 22.</b> YM-155 sensitizes NB MYCN Amplified cell lines to chemotherapy VP-16.....	53

# CHAPTER 1

## 1. INTRODUCTION

### 1.1 NEUROBLASTOMA

Neuroblastoma (NB) is the most common cancer diagnosed in the first year of life, accounting for 15% of cancer-related mortality in children, and ranking the most common solid malignancy found extracranially in pediatrics (Maris, 2010). NB is an embryonal tumor of the sympathetic nervous system, thought to be a precursor cell derived from neural-crest tissues- typically in the adrenal medulla or paraspinal ganglia (Maris, 2010; Smith and Foster, 2018). NB risk is classified in three ways; low, intermediate, or high; low- and intermediate-risk patients typically have a favorable outcome (~80%–95% event-free survival rate), but high-risk patients have <50% event-free chance of overall survival, and there is also a subset of “ultra-high” risk patients who do not respond to therapy (Huang and Weiss, 2013).

Current therapies of NB have significant long-term side effects and are highly toxic to healthy cells like chemotherapies, hence, it is critical to identify genetic factors and molecular pathways involved in driving NB pathogenesis and develop specific therapies for high-risk NB to achieve higher efficacy and to alleviate adverse effects (Guan *et al.*, 2017; Sun *et al.*, 2017). NB is associated with certain genetic markers that are used to identify risk, like MYCN, a member of the MYC gene family and encodes N-MYC protein, a transcription factor with a basic helix-loop-helix-leucine zipper domain, whose overexpression is indicative of aggressive disease and poor prognosis in NB patients (Huang and Weiss, 2013; Yi *et al.*, 2021). Heritable abnormalities in genes that regulate

cell division, proliferation, and death causes cancer, and such critical genetic factors underlying NB onset and progression include amplification of MYCN, and deletions of TP53 (Fetahu and Taschner-Mandl, 2021).

## **1.2 p53**

p53 is a nuclear phosphoprotein, that is usually present at low levels in the cells, due to a short half-life of approximately 30 min, but accumulates in response to cellular stress such as DNA damage from irradiation, and is tightly regulated by MDM2. MDM2 binds to p53, blocking its transcriptional function and targeting it for ubiquitin mediated degradation, thereby creating an autoregulatory feedback loop to tightly regulate p53 levels (Tweddle *et al.*, 2003). The process of malignant transformation universally entails genetic damage and oncogenic signaling, two stresses that are signaled to p53 through different genetic pathways which are the basis on which the two roles of p53 are distinguished. The first being “guardian of the genome”- sensing and reacting to DNA damage through the ATM/ATR and Chk1/Chk2 kinases, and the other, “policeman of the oncogenes”- responding to oncogenic signaling through the p53-stabilizing protein ARF (Efeyan and Serrano, 2007; **Figure 1**).

Abnormality in the p53 tumor suppressor gene pathway is an important mechanism of resistance to cytotoxic therapy. Tumors with predominantly wild-type p53 tend to be more chemo-responsive, e.g. testicular tumors whereas, tumors with mutant p53, respond less to chemotherapy, e.g. lung cancers (Tweddle *et al.*, 2003). In NB, there are few p53 mutations, of these the majority are in relapsed or progressive tumors, and the same report has been observed for NB cell lines with p53 mutations. Furthermore, in most cases the mutant cell lines are more chemo-resistant than wild-type cell lines. Transfection of wild-

type p53 NB cell lines leads to chemo-resistance, thereby supporting p53 inactivation as the mechanism involved (Tweddle *et al.*, 2003).

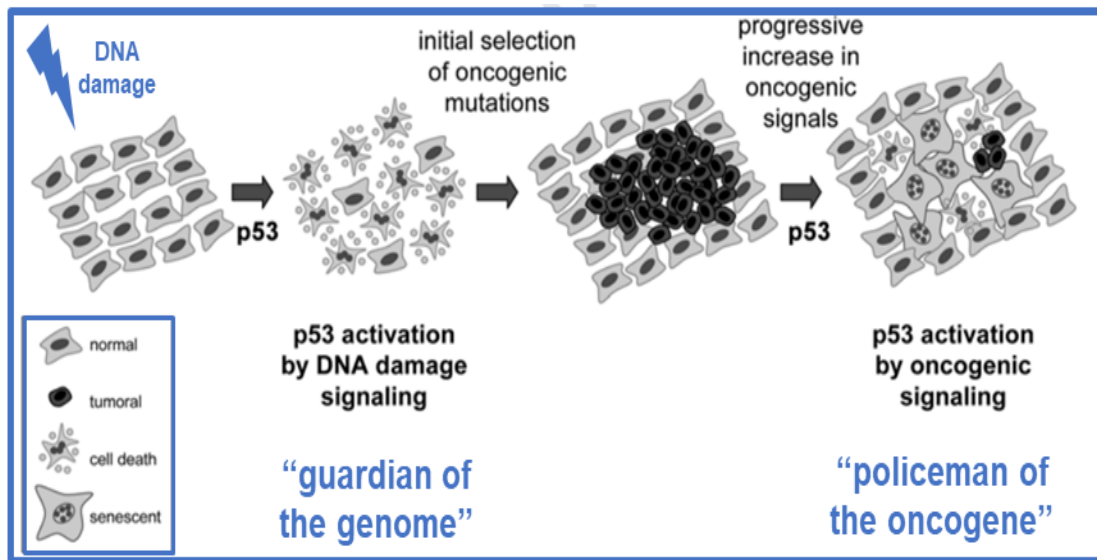


**Figure 1. The role of p53 during tumor progression.** p53 is activated by DNA damage signaling (“guardian of the genome”) and oncogenic signaling (“policeman of the oncogenes”). Cancer is initiated by DNA damage which general results in cell death. Damaged cells may carry oncogenic mutations and can generate an incipient tumor. Oncogenic signaling may increase through the accumulation of additional alterations and may result in cell death or senescence. Hypothetical survivor cells may mature to full malignancy. (Adapted from Efeyan and Serrano, 2007)

Additionally, another mechanism of p53 inactivation, and MDM2 amplification has also been reported in NB tumors at relapse and in associated tumor derived cell lines. These tumors are more chemo-resistant than wild-type p53 cell lines and p53 function is attenuated, and deletion of the p14ARF gene is an alternative mechanism of p53 inactivation and has been reported in three NB cell lines established post-treatment (Tweddle *et al.*, 2003). Notably, there is a stress-dependent reversal of the p53-dependent suppression of survivin expression in cells exposed to replication stress. That is, p53 becomes necessary to induce survivin, and this occurrence is interpreted as a fail-safe mechanism that facilitates both cellular repair processes and regular mitosis in p53 proficient cells. Moreover, if the damage is persistent or too severe, such cells can still undergo the p53-dependent apoptosis program preventing transformation (Rauch *et al.*, 2014).

### **1.3 SURVIVIN (BIRC5)**

Survivin protein, also known as baculoviral inhibitor of apoptosis repeat (BIR)-containing 5 (BIRC5) is encoded by BIRC5 gene and comprises of 142 amino acids with a single N-terminal Zn<sup>2+</sup>-binding BIR domain and a C-terminal with  $\alpha$ -helix motif as seen in **Figure 2**.

Both domains are essential for its functions; the former binds the target proteins involved in the regulation of apoptosis and mitosis, whereas the latter contains a microtubule binding site that allows interactions between survivin and the cytoskeleton. Survivin is found ubiquitously distributed during embryonic and fetal developmental

stages (Frassanito *et al.*, 2019). Survivin is 16.5 kDa in size, making it the smallest member of the inhibitors of apoptosis family (IAPs), which antagonizes the induction of cell death.

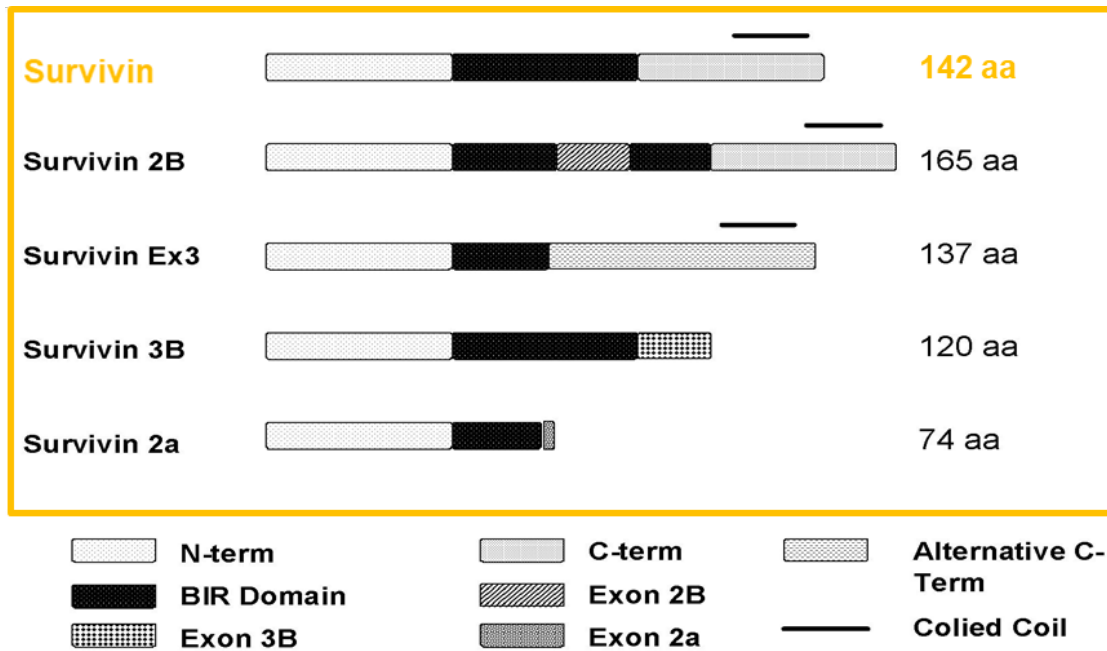


**Figure 2. Survivin structure.** (adapted from Duffy *et al.*, 2007). Representative diagram illustrating the structure of the five known variants of the survivin gene.

The multifunctional domains that constitute survivin allows for its involvement in several processes like various localization including interphase where survivin localizes to the cytoplasm and/or nucleus, in mitosis survivin is detected in the G2 phase, and it is also found extracellularly on the surface of exosomes which are constitutively secreted from cancer cells. Survivin is also involved in cellular functions such as cell death where survivin protects cells against apoptotic and autophagic death, and in mitosis where survivin; aids in ensuring that chromosomes are properly aligned prior to anaphase by targeting the chromosomal passenger complex to the centromeres during prometaphase, and the mitochondrial residence of survivin seems to be exclusively a cancer-associated phenomenon (Wheatley and Altieri, 2019).

Dysregulated expression of IAPs is frequently observed in cancers, and the high levels of survivin in tumors compared to normal adult tissues makes it an attractive target for pharmacological interventions (Rauch *et al.*, 2014). It has been shown in numerous studies that survivin, unlike other IAPs, is prominently expressed in many neoplasms but not in the differentiated normal tissue, and its overexpression has been demonstrated in various cancers: breast, lung, prostate, gastric, colon, bladder, esophageal carcinomas, osteosarcomas, and lymphomas. Survivin overexpression was also found to be significantly associated with a poor prognosis and decreased survival rates in oral, breast and colorectal cancers (Cheung *et al.*, 2013). The small imidazolium-based compound YM-155 has recently been reported to block the expression of survivin via inhibition of the survivin promoter, as seen in **Figure 3** (Rauch *et al.*, 2014).

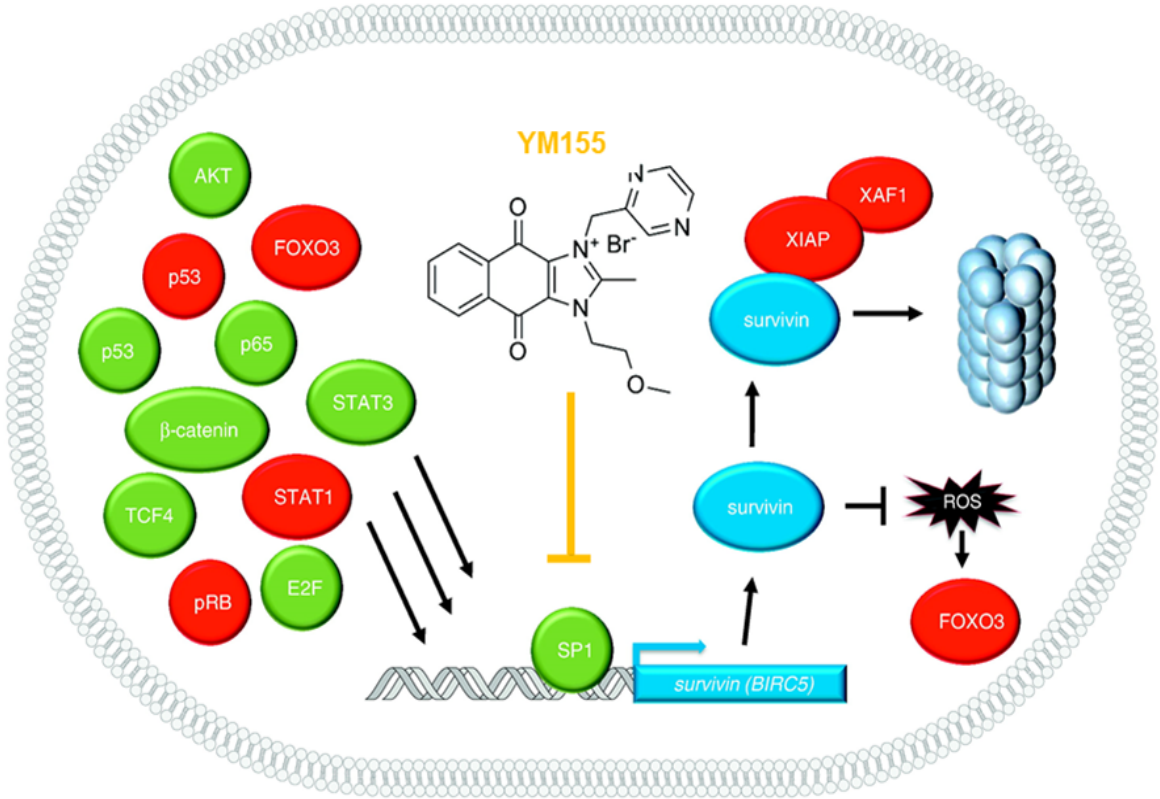


**Figure 3. Control of survivin expression at the mRNA and protein level.** (adapted from Rauch et al., 2014) Several transcription factors control survivin. Additionally, the proteasome restricts the stability of survivin. YM-155 blocks SP1 and this may reduce survivin expression.

#### **1.4 YM-155**

Sepantronium Bromide also commonly referred to as YM-155, is known to impair NB cell viability in clinically achievable concentrations via survivin depletion (Voges *et al.*, 2016). YM-155 is a small molecule compound originally developed as an expression suppressant of BIRC5 and it has reached Phase I/II clinical trials for the treatment of solid tumors, leukemia, and lymphoma (Cheng *et al.*, 2021). Pre-clinical studies showed that YM-155 suppressed both survivin protein and mRNA expression. Furthermore, in human studies, monotherapy with YM-155 has shown modest clinical activity with a tolerable safety profile in phase 1 and 2 trials in multiple cancer types (Kudchadkar *et al.*, 2015).

In the present study, YM-155 was used to inhibit NB progression. We investigated the effects of YM-155 on NB growth, and our results demonstrated that YM-155 specifically inhibits survivin, thereby promoting apoptosis. YM-155 was observed to significantly inhibit NB cell proliferation, colony growth, and 3D spheroid formation. Moreover, YM-155 induces apoptosis, block cell cycle progression, and sensitizes NB to chemotherapy. Overall, this study indicates; 1) the function of survivin as a therapeutic target in NB, 2) that YM-155 is a potent inhibitor of NB growth, and 3) a novel, less-lethal, and more- efficacious therapeutic di-modal treatment strategy for NB using YM-155 with current chemotherapies.

## CHAPTER 2

### 2. MATERIALS & METHODS

#### 2.1 CHEMICALS & REAGENTS

Sepantronium Bromide-YM-155 >98% (HY-10194) and Idasanutlin- RG-7388 >98% (HY-15676) were purchased from MedChem Express LLC (Monmouth Junction, NJ, USA). Thiazolyl blue tetrazolium bromide (MTT) was procured from Thermo Fisher Scientific (Ward Hill, MA, USA). Etoposide (VP-16), Methanol (MeOH), Trypan Blue 0.4% Solution, Crystal Violet, eBioscience™ Annexin V-FITC Apoptosis Detection Kit (BMS500FI-300, Invitrogen), Click-iT™ Plus EdU Flow Cytometry Assay Kit (C10632, Invitrogen), and Corning Cell Culture Phosphate Buffered Saline (PBS) 1X were obtained from Fisher Scientific (Hanover Park, IL, USA). Dimethyl sulfoxide (DMSO), Normocin Antimicrobial Reagent, RPMI-1640 Cell Culture Media, and 0.25% Trypsin-EDTA (1X) were acquired from VWR International (Radnor, PA, USA). Primary Antibodies: Survivin (71G4B7; 2808S) Rabbit mAb, p53 Rabbit mAb Antibody,  $\beta$ -Actin (4967) Rabbit mAb Antibody; and the Secondary Antibodies: anti-rabbit IgG HRP-linked secondary antibody (7074S), were purchased from Cell Signaling Technologies (Danvers, MA). The following primers: BIRC5, TP53, BCL-2, NOXA, MYCN, and PUMA (**Table 1.**) were purchased from GeneWiz LLC (South Plainfield, NJ, USA). Clarity™ Western ECL Substrate-Clarity Western Peroxide Reagent and Clarity Western Luminol/Enhancer Reagent were obtained from Bio-Rad Laboratories Inc. (Hercules, CA). Fetal Bovine Serum (FBS) Heat-Inactivated at 56C was acquired from Atlanta Biological (Flowery Branch, GA, USA). Corning Penicillin Streptomycin Solution, 100X, and L-glutamine Solution 200nM were purchased from Media Tech, Inc. (Manassas, VA, USA). RNeasy Mini Kit was acquired

from Qiagen (Valencia, CA, USA). Arium® mini plus UV Bench Top System US  
 Ultrapure Water was purchased from Sartorius (Bohemia, NY, USA).

<b><u>Gene</u></b>	<b><u>Primer</u></b>	<b><u>Sequence</u></b>
BIRC5	survivinB-F survivinB-R	GATGACGACCCCATAGAGGAAC CGCACTTTCTCCGCAGTTT
TP53	TP53-F TP53-R	CAGTTGGGCAGCTGGTTAGG ATCCTCCAGGGTGTGGGATG
BCL-2	BCL-2-F BCL-2-R	GTGGATGACTGAGTACCTGAAC GAGACAGCCAGGAGAAATCAA
NOXA	Noxa-F Noxa-R	TACCGCTGGCCTACTGTGAA ATGTGCTGAGTTGGCACTGA
PUMA	Puma-F Puma-R	GCGATTGCGATTGGGTGAGA TACTTCCTGCCCTGCTCTGG
GAPDH	GAPDH-F GAPDH-R	CACCATCTTCCAGGAGCGAG TGATGACCCTTTTGGCTCCC

**Table 1: Primers used to perform gene expression experiments.** Primers for gene expression analysis by quantitative real time RT-PCR.

## **2.2 CLINICAL PATIENT DATASETS**

Clinical patient datasets were analyzed using R2: Genomic Analysis and Visualization Platform (<https://hgserver1.amc.nl/cgi-bin/r2/main.cgi>) which supports multi-parametric analysis of NB patient outcomes with gene expression. Three patient datasets; Versteeg dataset (N=88), Kocak dataset (N=649), and SEQC dataset (N=498) were analyzed, with a total of 1235 primary NB patients. These publicly available datasets contain microarray profiles of unique primary tumors and were specifically examined for overall survival correlation and gene expression.

## **2.3 CELL CULTURE & MAINTENANCE**

Six groups of human NB cell lines; three MYCN Non-amplified (SH-SY5Y, SK-N-AS, CHLA-255) and three MYCN Amplified (NGP, LAN5, IMR-32), were routinely cultured and maintained as described previously (Agarwal *et al.*, 2015). Dr. Leonid Metelitsa of Baylor College of Medicine, Houston graciously provided CHLA-255 cell lines (Agarwal *et al.*, 2016). All cell lines were maintained in RPMI-1640 media (Lonza, MD) supplemented with 10% FBS, 1% penicillin/streptomycin, 1% L-glutamine, and 0.2% normocin, at 37°C, with 5% CO<sub>2</sub> in a humidified incubator (New Brunswick, Eppendorf Galaxy 170 R).

Cell lines were sub-cultured for maintenance and used in experiments with the following technique: 5mL of 1X PBS was used to wash the cells then aspirated, trypsinization followed with 1.5mL 0.25% Trypsin-EDTA (1X) for 75cm<sup>2</sup> flasks and 4.5mL for 175cm<sup>2</sup> flasks and incubated at 37°C for 3 minutes, cells were checked under the Leica DMI1 Inverted Microscope to ensure cells were completely detached from the flask surface, neutralization followed with 8mL RPMI-1640 media per 1.5mL of trypsin,

then centrifuged at 400rpm for 5 minutes at room temperature using a Beckman Coulter Allegra X-14R Centrifuge, the supernatant was aspirated and the cells were resuspended with 5mL 1X PBS and mixed well, then a 10 $\mu$ L aliquot of cell suspension was mixed with 10 $\mu$ L trypan blue, and a 10 $\mu$ L of the mixture was loaded onto a Bio-Rad counting slide and inserted into a Bio-Rad TC-20 Automated Cell Counter for cell counting. The stock cell suspension was centrifuged at 400rpm for 5 minutes, then resuspended in RPMI-1640 supplemented media and seeded at varying densities according to the experiment being performed. In the case of cell culture maintenance, 1x10<sup>6</sup> cells were seeded in 13mL of media or, 2x10<sup>6</sup> cells were seeded in 21mL of media for 75cm<sup>2</sup> and 175cm<sup>2</sup> flasks respectively.

#### **2.4 PREPARATION OF DRUG TREATMENT SOLUTIONS**

The main YM-155 stock solution of 10mM was prepared by adding 1.13mL of DMSO to the 5mg vial of YM-155 powder and divided into smaller aliquots in 1.5mL tubes then stored at -80°C. The working stock solution of 10mM was then used to make a serial dilution of 1mM, and the 1mM aliquot was used to make a serial dilution of 100 $\mu$ M. All serial dilutions were prepared using DMSO and all working stock solutions were stored in -20°C. All treatment solutions of YM-155 were prepared fresh on the day of use or used within 1 week of preparation in RPMI-1640 supplemented media using a fresh aliquot of YM-155 working solution. The calculations of drug and media to be added for the desired concentrations were recorded and used. Each treatment solution was prepared by aliquoting the volume of media required, followed by the corresponding volume of drug, based on the desired concentration. The control for every experiment treatment, was RPMI-1640 supplemented media alone.

## **2.5 CELL VIABILITY USING MTT ASSAY**

Cell viability assays were performed using MTT powder, 98%. The six NB cell lines were seeded at various densities as follows:  $9 \times 10^3$  for CHLA-255, NGP and IMR-32, then  $1 \times 10^4$  for SH-SY5Y, SK-N-As and LAN-5 cells per well in 96-well plates and at ~70% confluency were treated with different concentrations of YM-155 for 72 hours. The highest concentration of  $64 \mu\text{M}$  was made using the  $10 \text{mM}$  working stock, and then serial 1:4 dilutions were performed using DMSO, for the next seven concentrations up to  $0.00390625 \mu\text{M}$ . Next,  $20 \mu\text{L}$  of  $5 \text{mg/mL}$  MTT solution (MTT powder and deionized water from Arium® mini plus UV Bench Top System US Ultrapure Water) was added to each well without removing the treatment media and incubated for 4 hours at  $37^\circ\text{C}$ , with 5%  $\text{CO}_2$  in a humidified incubator. At the end of the incubation, the treatment media containing MTT was removed by sharply inverting the plate once and resuspended the formazan (MTT metabolic product) in  $100 \mu\text{L}$  of DMSO. The plates were then placed on a VWR Microplate Shaker for 5 mins at 300rpm, and then analyzed by spectrophotometric absorbance at 560nm optical density and minus background at 670nm using a microplate reader (SpectraMax iD3, Molecular Device). The data obtained was analyzed using Microsoft Excel and the cell viability was determined by comparing the average absorbance reading of respective treatment concentrations minus average blank absorbance to, average control absorbance readings minus average blank absorbance, and reported as percentage viability of control. The data represents mean percent of control for three or four experiments, each performed with three replicates.  $\text{IC}_{50}$  values were calculated using GraphPad Prism 8 software.

## **2.6 CLONOGENIC ASSAY**

Clonogenic assays were performed using 0.2% Crystal Violet Solution. First, 2mL of  $2.5 \times 10^3$  NB cells were seeded per well into 6-well plates for all six cell lines previously mentioned and incubated at 37°C, with 5% CO<sub>2</sub>, in a humidified incubator. After 24 hours, the media was removed and 2ml fresh treatment media was added. Different concentrations of YM-155 were used, with at least two replicates per concentration. After 48 hours, the treatment media was removed, and 2mL of fresh media was added to each well and the plates were incubated for approximately 10-12 days when the control treatment wells became confluent. After the incubation period was finished, the plate was placed on ice for 10minutes before the media was removed from each well, then the colonies were stained by adding 500µL freshly prepared ice-cold 0.2% crystal violet solution to each well and removed from the ice and incubated at room temperature in the dark for 30minutes. The plate was then washed by dipping once in a 1000mL beaker of water and the plate was put upside down on a Kimwipe to air dry. Each dried plate was then visualized and counted manually. All assays were performed in triplicates and repeated at least three times with appropriate controls. 0.2% Crystal violet was prepared by adding 100mg of crystal violet to 25% Methanol (12.5mL Methanol + 37.5mL Deionize water), the mixture was vortexed, filtered (used 0.2mm sterile syringe filter & 20mL syringe), labelled and was then ready to be used.

## **2.7 3D-SPHEROID ASSAY**

3D spheroid assays for NB were performed using round bottom 3D spheroid 96-well plates (4515; Corning). NB cells from two cell lines- SH-SY5Y and IMR-32, were seeded at a density of  $5 \times 10^3$  cells/well in 200µL media per well, then centrifuged (7

minutes, 1000rpm, 21°C) and incubated in a humidified incubator (at 37°C, with 5% CO<sub>2</sub>), for two days to develop spheroids with diameters of approximately 300µm. Spheroids with diameters of 300µm or 300µm ± 2µm were selected and treated by removing 100µL of media without disturbing the spheroid and adding 100µL of fresh treated media for the following concentrations of YM-155: Control (media only), 1mM, 5mM, and 10mM. Treatment continued for the next 12 days with constant replenishment of the drug every three days. Spheroid images were captured consistently before each treatment and on day 12, using Leica DMi1 microscope, and the spheroid size (diameter length) was determined using the LASX software suite (Leica Microsystems). On day 12, after imaging, the viability of the spheroid cells was measured utilizing the Viability/Cytotoxicity Assay Kit for Animal Live & Dead Cells (3002; Biotium Inc.). The contents of the assay kit- Calcein AM and Ethidium homodimer III (EthD-III) dyes were then thawed on ice and used to prepare a staining solution of 2mM and 4mM EthD-III which was then vortexed. Momentarily, 100µL of media was removed from each well, and replaced with 100µL of staining solution without disturbing the spheroids. The stained spheroids were imaged and analyzed using the EVOS FL imaging system (Thermo Scientific). After which, the fluorescence was quantified using a microplate reader (SpectraMax iD3, Molecular Device) at 517nm for the Calcein AM dye and at 625nm for the EthD-III dye. Additionally, the 3D spheroid viability was determined using the CellTiter-Glo® 3D Cell Viability Assay (G9683; Promega). Briefly, 100µL of media and staining solution were removed from each well, and replaced with 100µL of 3D reagent, then the contents were mixed vigorously by pipetting up and down to induce cell lysis and incubated for 30 minutes

followed by quantifying the luminescence using a multi-mode microplate reader (SpectraMax iD3, Molecular Device).

## **2.8 APOPTOSIS ASSAY**

Apoptosis in NB cell lines was analyzed using the eBioscience™ Annexin V-FITC Apoptosis Detection Kit (BMS500FI-300, Invitrogen). NB cells from two cell lines- SH-SY5Y and NGP, were seeded using 6-well plates at a density of  $2.5 \times 10^5$  cells/well in 2mL media per well and incubated for 24 hours in a humidified incubator. NB cells of ~70% confluency were treated with fresh media for the following three concentrations of YM-155- Control (media only), 1mM, and 5mM, for 16 hour, then washed with cold PBS and resuspended with 200 $\mu$ L of binding buffer(1X). Next, 10 $\mu$ L of Annexin V-FITC was added to 190 $\mu$ L cell suspension, mixed and incubated for 30 minutes at room temperature. Cells were then washed in 200 $\mu$ L of binding buffer (1X) and resuspended in 190 $\mu$ L binding buffer (1X). Finally, 10 $\mu$ L Propidium Iodide (20 $\mu$ g/mL) was added and the samples were analyzed using Attune NxT Acoustic Focusing Cytometer (A24861, Life Technologies).

## **2.9 CELL CYCLE ASSAY**

The cell cycle analysis in NB cells was performed using the Click-iT™ Plus EdU Flow Cytometry Assay Kit (C10632, Invitrogen). NB cells from two cell lines- SH-SY5Y and NGP, were seeded using 6-well plates, at a density of  $2.5 \times 10^5$  cells/well in 2mL media per well and incubated for 24 hours in a humidified incubator. NB cells of ~70% confluency were then treated with fresh media for the following three concentrations of YM-155- Control (media only), 1mM, and 5mM, for 16 hours. First, the cells were labelled with Click-iT™ EdU, then EdU was added to yield a final concentration of 10 $\mu$ M per well, and then the plate was incubated for 1 hour at 37°C. Cells were then harvested using 300 $\mu$ L

trypsin, 2mL media and 1X PBS to wash, and collected into 6 labelled tubes (1 unstained, 1 Click-iT, 1 Fx, 1 Both-Click-iT/Fx, and 2 controls). The cells were then fixed and permeabilized; the cells in the “Click-iT”, and “both” tubes were first washed with 1mL 1% BSA then with 1mL 1X PBS, and centrifuged (400rpm for 5 minutes) followed by removing the supernatant. The pellet was dislodged, mixed well with 100µL Click-iT fixative (4% paraformaldehyde in PBS), and then incubated at room temperature for 15 minutes, in the dark. The cells were washed with 1mL 1% BSA then in 1mL 1X PBS, and centrifuged (400rpm for 5 minutes) followed by removing the supernatant. The pellet was dislodged, resuspended in 100µL 1X Click-iT permeabilization & wash reagent, mixed well, and incubated for 15 minutes. Next Click-iT EdU was detected; the Click-iT Plus reaction cocktail was prepared for 3 reactions according to manufacturer’s recommendations and must be used within 15 minutes of preparation (1.313mL 1X PBS, 30µL copper protectant (100mM aqueous solution), 7.5µL fluorescent dye picolyl azide, and 150µL 10X reaction buffer additive). Then, 0.5mL of Click-iT Plus reaction cocktail was added to each tube of fixed cells and mixed well- total volume for each reaction mix was 600µL(100+500µL). The reaction mixture was then incubated for 30 minutes at room temperature in the dark then centrifuged. The cells were then washed with 1mL 1X Click-iT permeabilization & wash reagent, centrifuged and the supernatant was removed. The pellets for the Click-iT/Fx sample and the Fx only samples were resuspended in 500µL FxCycle™ PI/RNase staining solution and incubated for 30 minutes. Finally, the samples were analyzed using Attune NxT Acoustic Focusing Cytometer (A24861, Life Technologies) at 488 nm excitation with a green emission filter (530/30nm).

## **2.10 RNA EXTRACTION, cDNA SYNTHESIS and QUANTITATIVE RT-PCR**

Total RNA was extracted, and cDNA was synthesized from NB cells by using a RNeasy plus mini kit (74134; Qiagen), and high-capacity cDNA reverse transcription kit (4368814; Applied biosciences) respectively, according to the manufacturer's instructions. NB cells from SH-SY5Y cell line, were seeded using 6-well plates, at a density of  $1 \times 10^6$  cells/well in 2mL media per well and incubated for 24 hours at 37°C. NB cells of ~70% confluency were treated with fresh media and YM-155 for three concentrations- Control (media only), 1mM, and 5mM, for 6 hours. In step 1) the RNA was extracted; the cells were harvested by using 300 $\mu$ L trypsin, 2mL media and 1X PBS to wash, then centrifuged. The supernatant was removed, then the cell pellet was stored on ice, and 350 $\mu$ L Buffer RLT plus with  $\beta$ -ME ( $\beta$ -mercaptoethanol) was added to the cell pellet and vortexed for 30 seconds. The homogenized lysate was then transferred to a gDNA eliminator spin column placed in a 2mL collection tube and centrifuged for 30 seconds at 10,000rpm in 4°C using a Beckman Coulter Micro-Centrifuge (MRB19A012). The column was discarded and 350 $\mu$ L of 70% ethanol was added to the flow-through and mixed well. Then, 700 $\mu$ L of the sample was transferred to a RNeasy spin column, placed in a 2mL collection tube, centrifuged (15 second, 10,000rpm, 4°C), and the flow-through was discarded. Next, 700 $\mu$ L of buffer RW1 was added to the RNeasy mini spin column in a 2mL collection tube, the lid was closed, it was centrifuged (15 second, 10,000rpm, 4°C), and the flow-through discarded. After which 500 $\mu$ L of buffer RPE was added to the RNeasy spin column, the lid was closed, the column centrifuged (15 second, 10,000rpm, 4°C), the flow-through was discarded, and this was repeated once to dry the column membrane, then a new 2mL collection tube was used and centrifuged (1 minute, 15,000rpm, 4°C) to further dry the

membrane. The RNeasy spin column was then placed into a new 1.5mL collection tube, and 30 $\mu$ L RNase-free water was added directly to the spin column membrane, the lid was closed, it was centrifuged (1 minute, 10,000rpm, 4°C) and the RNA was eluted. The amount and purity of the extracted RNA was determined spectrophotometrically at 260nm using (NanoDrop OneC, ThermoFisher Scientific)- the instrument was blanked using 1 $\mu$ L RNase-free water, then 1 $\mu$ L of each sample was read with cleaning in between reads with 70% ethanol. The amount of RNA in each sample was then normalized using RNase-free water to 2000 ng of RNA in each 10 $\mu$ L total sample per concentration. In step 2) cDNA was synthesized from RNA; RNA was reverse transcribed into cDNA using the high-capacity cDNA reverse transcription kit (4368814; Applied biosciences) as per the protocol provided by the manufacturer; the kit components were thawed on ice then used to prepare the 2X RT master mix for 3 samples using them in this order; 6 $\mu$ L 10X RT buffer, 2.4 $\mu$ L 25X dNTP mix (100mM), 6.0 $\mu$ L 10X random primers, 9.6 $\mu$ L nuclease-free water, 3.0 $\mu$ L RNase inhibitor, and 3.0 $\mu$ L MultiScribe™ Reverse Transcriptase- the total reaction volume was 30 $\mu$ L. The 2X RT master mix was placed on ice, mixed gently, and 10 $\mu$ L was added to each sample. The samples were then loaded on the MiniAmp™ Plus Thermo Cycler (2280318081463, Applied Biosystem) for 2 hours and 16 minutes, and the result was cDNA. Utilizing the cDNA prepared from NB cells, the RT-PCR reactions were performed for five (5) individual genes (BIRC5, TP53, BCL-2, NOXO, and PUMA) in triplicate using the SYBR Green master mix (4385610; ThermoFisher Scientific) on a QuantStudio 3 Real Time PCR System (ThermoFisher Scientific). The relative expression was normalized by using GAPDH as a house keeping gene, and the *p*-values were calculated by Student's *t*-test to determine the expression-fold difference of individual genes.

## **2.11 IMMUNOBLOTTING ASSAYS**

Immunoblotting assays were performed as described previously (Agarwal *et al.*, 2018). NB cells from NGP cell line, were seeded using 100 x 22mm (60.8cm<sup>2</sup>) cell culture dishes, at a density of 3x10<sup>6</sup> cells/well in 10mL media per dish and incubated for 24 hours at 37°C, with 5% CO<sub>2</sub>, and 19% O<sub>2</sub> in a New Brunswick by Eppendorf company Galaxy 170 R humidified incubator. NB cells of ~70% confluency were then treated with fresh media and YM-155 at three concentrations- Control (media only), 0.25µM, 0.5µM and 0.75µM, for 24 hours. In another study which combined YM-155 with RG-7388 the treatment concentrations were Control (media only), 0.25µM-RG, 0.5µM-YM, 1µM-YM, 0.25/0.5µM-RG/YM, and 0.25/1µM-RG/YM, and the incubation period was for 24 hours at the same conditions previously mentioned. Briefly, total proteins were extracted by lysing cells in RIPA extraction and lysis buffer (89900; ThermoFisher Scientific) supplemented with protease inhibitor cocktail (Complete mini EDTA free, Roche) and phosphatase inhibitor cocktail (PhosSTOP, Roche). Cell lysates were collected after centrifuging for 15 minutes at 15,000rpm followed by protein quantification using the Bradford assay according to the manufacturer's instructions (5000205; Bio-Rad). Equal amounts of 7.5µg protein samples were separated on 4-12% SDS-PAGE gels, transferred to PVDF membrane (Bio-Rad), blocked with 5% BSA solution, and probed with the indicated primary antibody overnight at 4°C on a rocker. The membrane was then washed and incubated with either anti-mouse or anti-rabbit IgG HRP-conjugated secondary antibody for 2 hours at room temperature. Blots were then developed using the Clarity ECL Western substrate (Bio-Rad), visualized, imaged, and documented using the ChemiDoc XRS Plus system (Bio-Rad).

## **2.12 SYNERGY STUDIES**

NB cells were seeded in 96-well plates and combination index (CI) studies were performed by treating cells with YM-155, VP-16, and their combination in a specific ratio. Cytotoxicity assays were then performed as described above followed by calculation of the CI values and dose-reduction indices (DRIs) by using the Chou-Talalay method for drug interactions using CompuSyn software for the different fractions affected (38).  $CI < 1$ ,  $= 1$ , and  $>1$  indicates synergism, additive effect, and antagonism, respectively.  $DRI >1$ , and  $<1$  indicates a favorable and an unfavorable dose-reduction, respectively.

## **2.13 STATISTICAL ANALYSIS**

In the present study, assays were performed with at least three technical replicates, and experiments were repeated at least thrice, and representative results are presented. All values are presented as the mean  $\pm$  standard deviation (SD). A two-tailed Student's t-test was used to determine the statistical significance among drug treatment groups.  $P < 0.05$  was considered statistically significant. Patient survival analyses were performed using the Kaplan-Meier method and two-sided log-rank tests. The  $IC_{50}$  value was calculated with GraphPad Prism 8 software.

## CHAPTER 3

### 3. RESULTS

#### 3.1 BIRC5 EXPRESSION CORRELATES WITH POOR NB PROGNOSIS

To perform an investigation on how the transcription of BIRC5 correlates with NB patient outcomes, we analyzed the clinical results of 1235 NB patients using the R2-patient database platform. Kaplan-Meier survival analysis revealed that high expression of BIRC5 leads to poor prognosis, for Kocak dataset (N=649, BIRC5 p=1.3e-23), SEQC dataset (N=498, BIRC5 p=5.3e-21), and Versteeg dataset (N=88, BIRC5 p=6.1e-07) (**Figure 4 A-C**).

Furthermore, aggressive, and higher stage tumors had significantly higher BIRC5 expression, as well as higher levels of BIRC5, suggesting that BIRC5 plays a substantial role in NB progression (**Figure 5 A-C**). We also observed significantly higher expression of BIRC5 in the three datasets Kocak p=4.31e-33, SEQC p=7.56e-25, and Versteeg p=6.72e-05) in highly aggressive MYCN Amplified tumors in comparison to MYCN Non-amplified tumors (**Figure 6 A-C**). In contrast, low expression of BIRC5 strongly correlates with better overall survival as well as event-free survival of NB patients. These findings suggested that BIRC5 is a critical predictive factor for NB patients.

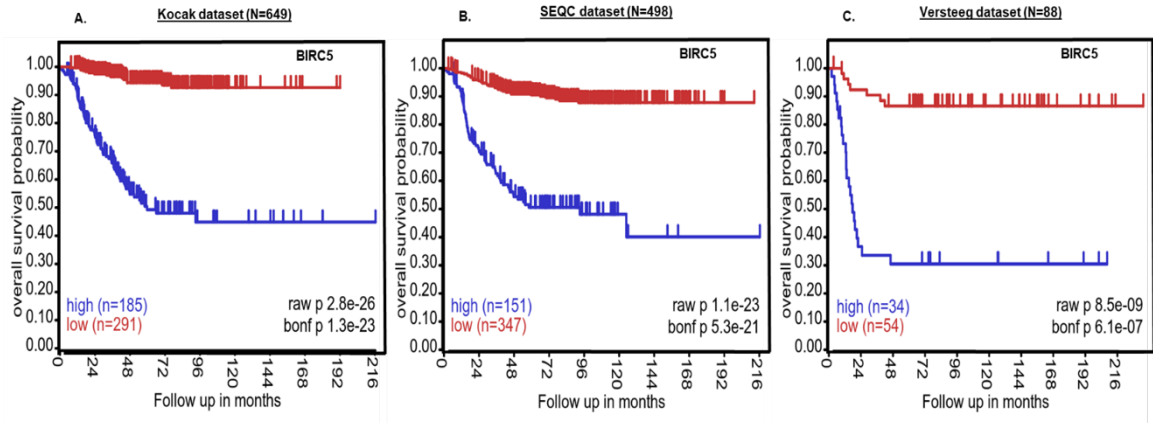


**Figure 4: BIRC5 expression correlates with poor overall survival of NB patients.** Kaplan-Meier analysis in response to BIRC5 gene expression showing overall probability of NB patients' survival. **(A)** Kocak dataset of 649 patients. **(B)** SEQC dataset of 498 patients. **(C)** Versteeg dataset of 88 patients. (N=1235)

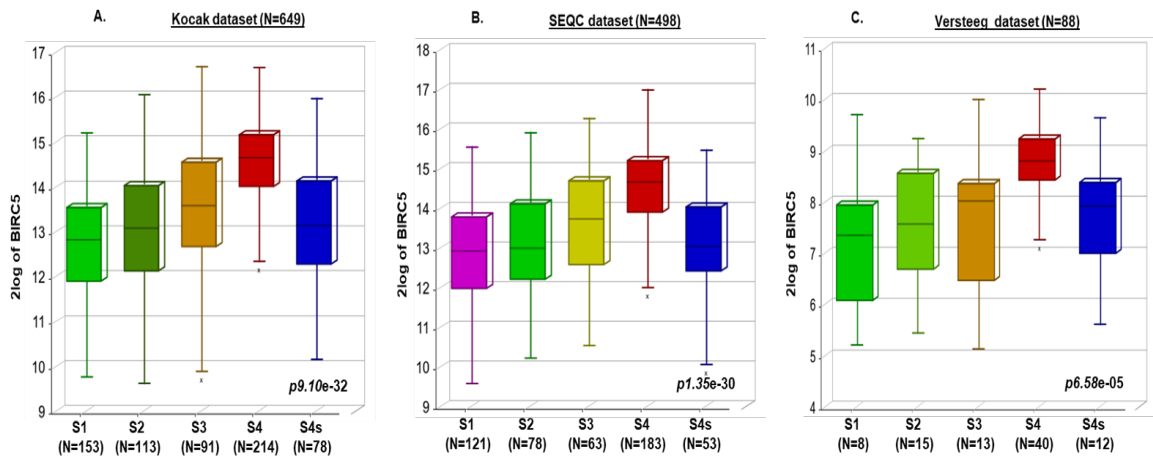


**Figure 5: BIRC5 expression correlates with NB progression.** Box-plot correlation analysis of NB stages as defined by International NB Staging System (INSS) in response to BIRC5 gene expression. **(A)** Kocak dataset of 649 patients. **(B)** SEQC dataset of 498 patients. **(C)** Versteeg dataset of 88 patients. (N=1235)

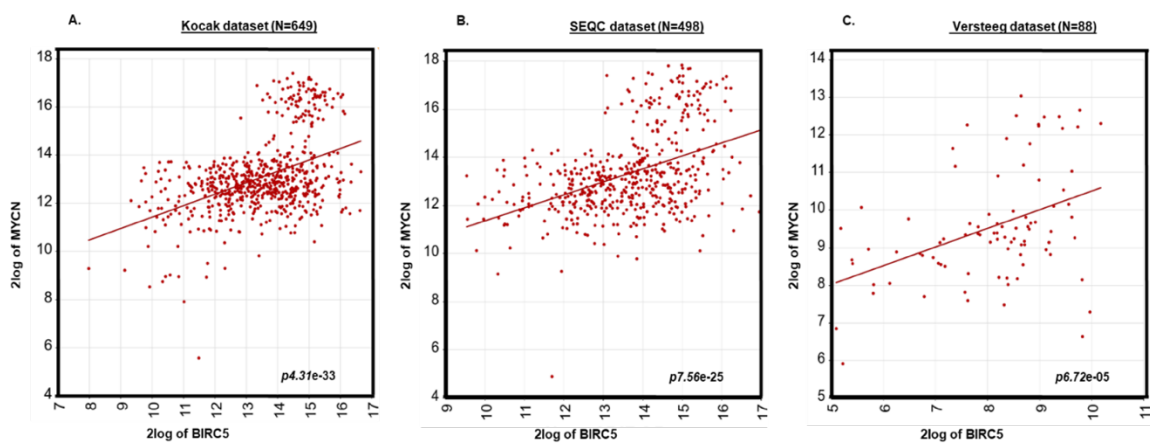


**Figure 6: BIRC5 expression correlates with MYCN Amplified cells and NB progression.** XY-plot correlation analysis of NB progression with respect to BIRC5 and MYCN gene expression. **(A)** Kocak dataset of 649 patients. **(B)** SEQC dataset of 498 patients. **(C)** Versteeg dataset of 88 patients. (N=1235)

### **3.2 YM-155 INHIBITS NB PROLIFERATION**

To determine the effects of inhibiting BIRC5 activation in NB, we utilized a small molecule survivin inhibitor, YM-155. We performed cytotoxicity assays in six (6) human NB cell lines including three MYCN Non-amplified (SH-SY5Y, SK-N-AS, CHLA-255) and three MYCN Amplified (NGP, LAN5, IMR-32), and treated with increasing concentrations of YM-155. The results obtained showed that YM-155 significantly inhibits NB cell proliferation in both MYCN Non-amplified and Amplified cell lines in a dose-dependent manner (**Figure 7 and 8**).

To further evaluate the anti-proliferative effect of YM-155 on NB, we performed clonogenic assays on six NB cell lines. Results showed that YM-155 significantly reduced the overall NB colony formation capacity in treated cells in contrast to the control cells in a dose-dependent manner (**Figure 9 and 10**).

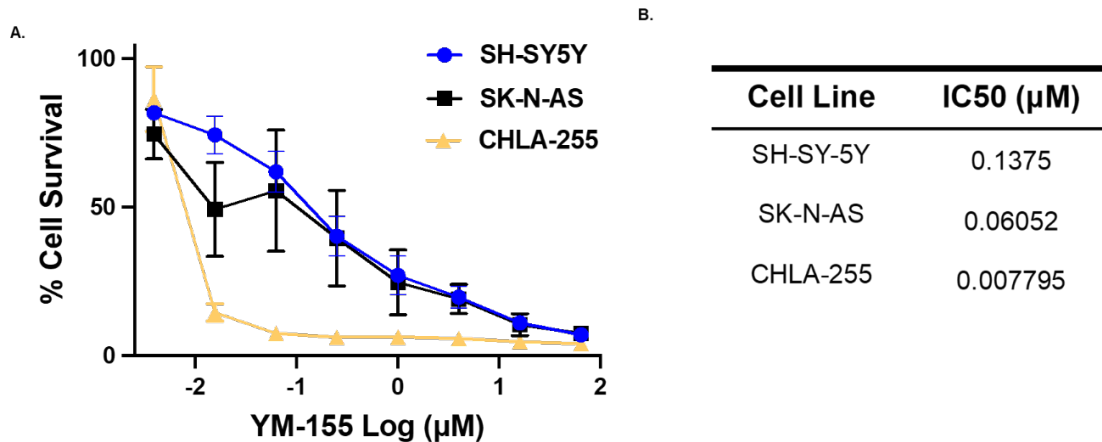


**Figure 7: YM-155 inhibits NB proliferation in MYCN Non-amplified cell lines. (A and B)** Cell cytotoxicity of YM-155 was measured using MTT dye reduction assay on six human NB cell lines. Three MYCN Non-amplified and three MYCN Amplified cell lines were treated with different concentrations of YM-155 at 72-hour time points. The absorbance of each well was measured at 560nm and plotted as a cell viability curve. **(A)** MYCN Non-amplified cell lines SH-SY-5Y, SK-N-AS, CHLA-255. **(B)** Summary table of IC<sub>50</sub> values calculated for three MYCN Non-amplified NB cell lines as shown in **Figure 7A**.

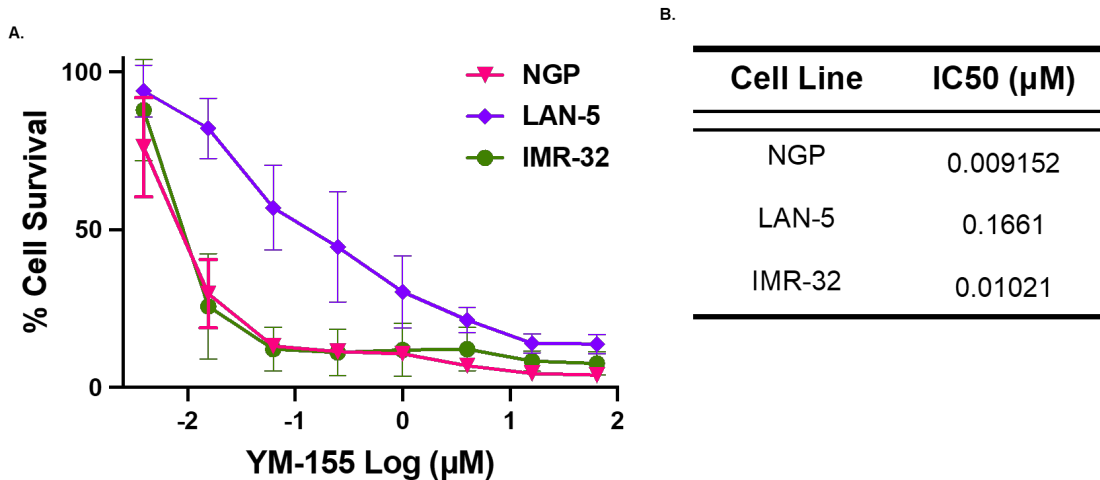


**Figure 8: YM-155 inhibits NB proliferation in MYCN Amplified cell lines. (A and B)**

Cell cytotoxicity of YM-155 was measured using MTT dye reduction assay on six human NB cell lines. Three MYCN Non-amplified and three MYCN Amplified cell lines were treated with different concentrations of YM-155 at 72-hour time points. The absorbance of each well was measured at 560nm and plotted as a cell viability curve. **(A)** MYCN Amplified cell lines NGP, LAN-5, IMR-32. **(B)** Summary table of IC<sub>50</sub> values calculated for three MYCN Amplified NB cell lines as shown in **Figure 8A**.

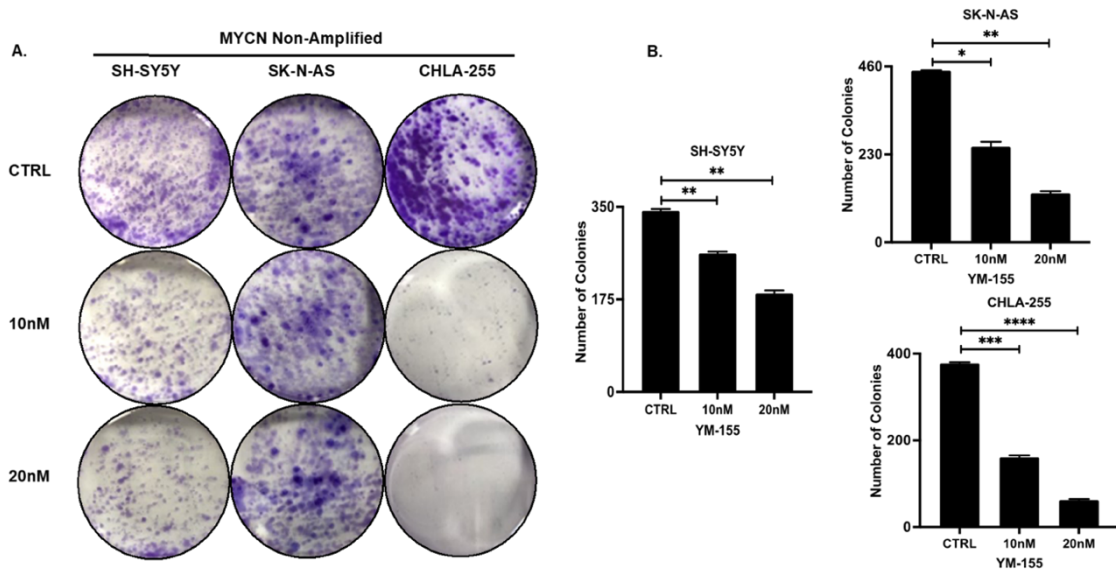


**Figure 9: YM-155 inhibits NB colony formation in MYCN Non-amplified cell lines.**

**(A and B)** Colony formation assay of NB cells treated with YM-155 in six cell lines- three MYN Non-amplified and three MYCN Amplified and stained with 0.2% Crystal Violet.

**(A)** Representative images of colony formation assay of NB cells when treated with YM-155 in three MYCN Non-amplified cell lines SH-SY-5Y, SK-N-AS, CHLA-255. **(B)** The colonies were counted and plotted. Survival index shows the quantitation of relative inhibition of colony formation of NB cells when treated with YM-155 seen in **Figure 9A**.

\*  $p < 0.05$ , \*\*  $p < 0.01$ , \*\*\*  $p < 0.001$ , \*\*\*\*  $p < 0.0001$

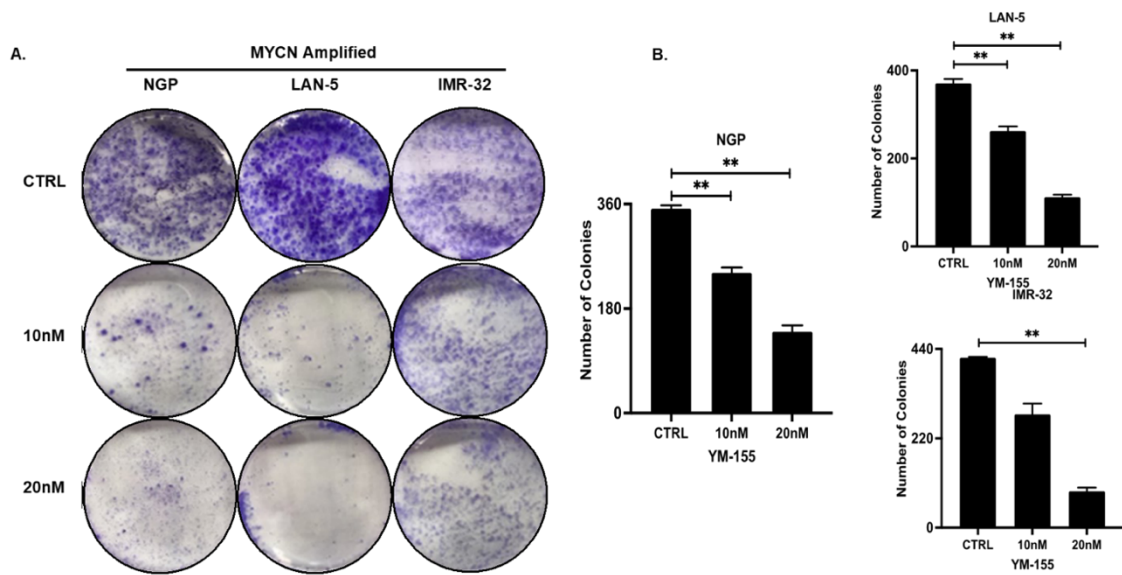


**Figure 10: YM-155 inhibits NB colony formation in MYCN Amplified cell lines.**

Colony formation assay of NB cells treated with YM-155 in six cell lines- three MYN Non-amplified and three MYCN Amplified and stained with 0.2% Crystal Violet. **(A)** Representative images of colony formation assay of NB cells when treated with YM-155 in three MYCN Amplified cell lines NGP, LAN-5, IMR-32. **(B)** The colonies were counted and plotted. Survival index shows the quantitation of relative inhibition of colony formation of NB cells when treated with YM-155 seen in **Figure 10A**. \*\*  $p < 0.01$

### **3.3 YM-155 INDUCES APOPTOSIS AND BLOCKS CELL CYCLE**

We further investigated the effects of YM-155 in inducing apoptosis in NB cells. Annexin V apoptosis assays in both MYCN Non-amplified SH-SY5Y and MYCN Amplified NGP NB cell lines showed that YM-155 significantly induced apoptosis in a dose-dependent manner. Specifically, YM-155 increased the percentage of Annexin V positive early apoptotic cells in comparison to the controls (**Figure 11**).

Furthermore, we observed that YM-155 inhibits cell cycle progression in SH-SY5Y and more significantly in NGP NB cells. YM-155 potently inhibits the S phase by blocking the G0/G1 to S transition, therefore increasing the percentage of cells in the G0/G1 phase (1.1-fold & 1.7-fold increase in SH-SY5Y & NGP respectively at 1 $\mu$ M, and 1.2-fold & 1.8-fold increase in SH-SY5Y & NGP respectively at 5 $\mu$ M), while decreasing the percentage of cells in the S phase (1.4-fold & 11.9-fold decrease in SH-SY5Y & NGP respectively at 1 $\mu$ M, and 1.6-fold & 22.2-fold decrease in SH-SY5Y & NGP respectively at 5 $\mu$ M), in comparison to controls (**Figure 12**). This data further suggests that YM-155 inhibits NB growth by promoting DNA synthesis (S) phase arrest and inducing apoptosis.

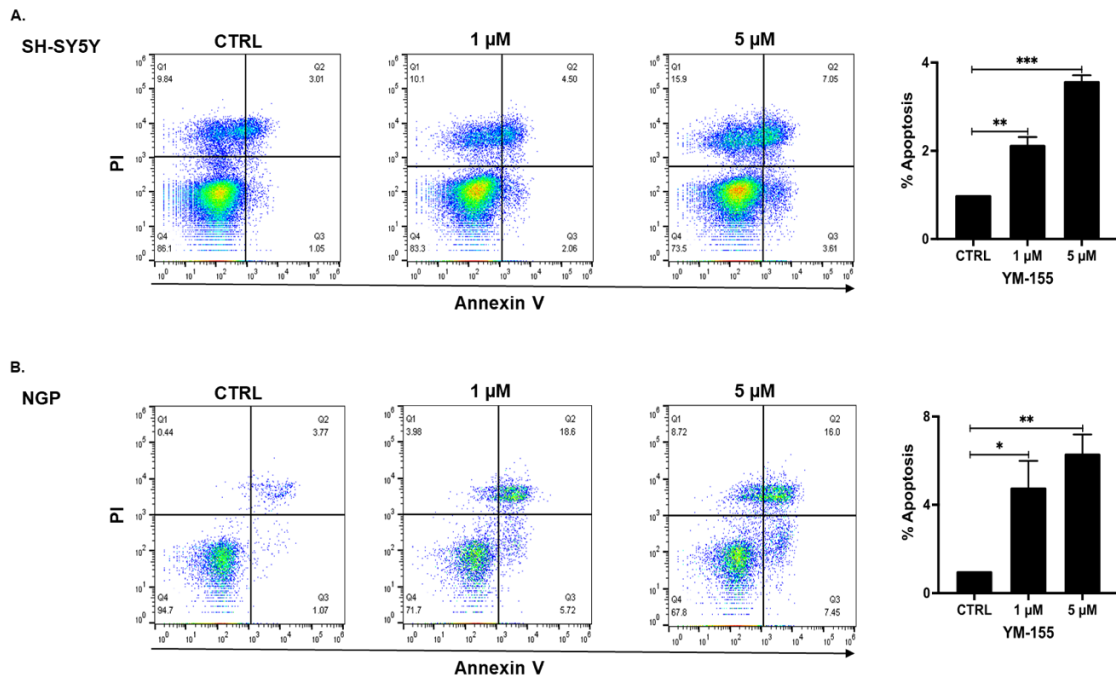


**Figure 11: YM-155 induces apoptosis in NB cells. (A and B)** YM-155 induces apoptosis in MYCN Non-amplified and MYCN Amplified NB cells. NB cells were treated with various concentrations of YM-155 (Control, 1 $\mu$ m, 5 $\mu$ m) for 16hrs. Representative Flow cytometer images and graphical representation of % Apoptosis are shown in **(A)** SH-SY5Y, and **(B)** NGP cell lines. \*p<0.05, \*\* p<0.01, \*\*\* p<0.001.

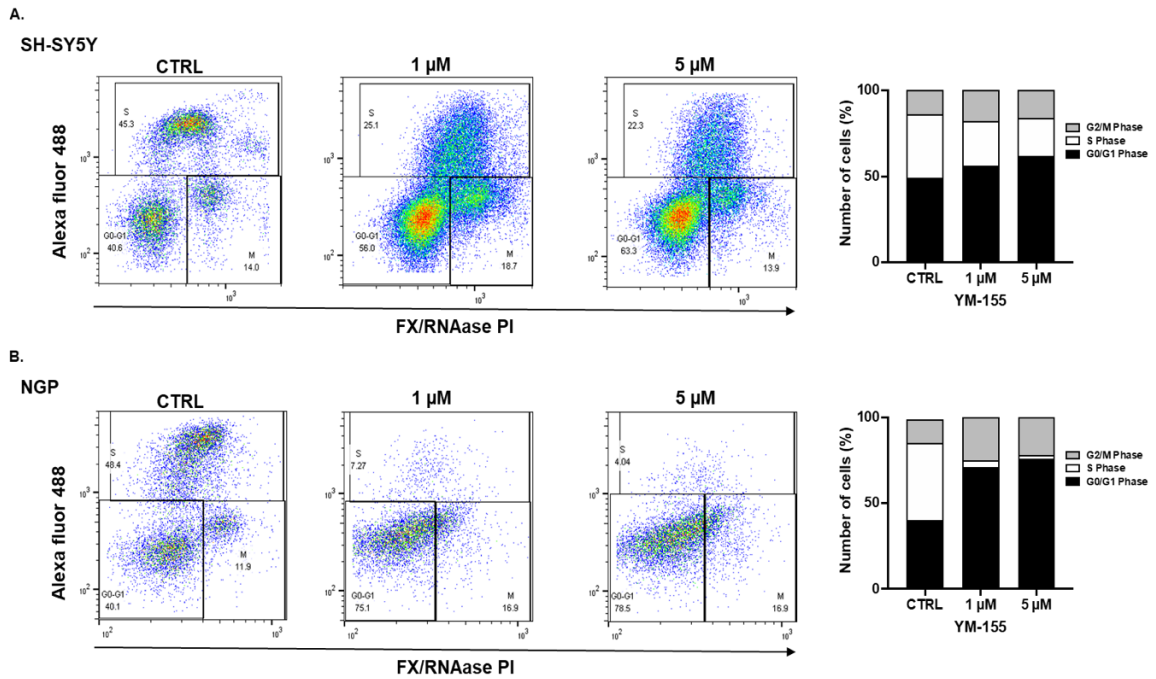


**Figure 12: YM-155 blocks cell cycle progression in NB cells. (A and B)** YM-155 blocks cell cycle in MYCN Non-amplified and MYCN Amplified NB cells. NB cells were treated with various concentrations of YM-155 (Control, 1 $\mu$ m, 5 $\mu$ m) for 16hrs. Representative Flow cytometer images and graphical representation of cell cycle analysis performed using cell cycle assay kit are shown in: **(A)** SH-SY5Y, and **(B)** NGP cell lines.

### **3.4 YM-155 INHIBITS NB SPHEROID GROWTH**

To mimic the physiological conditions of *in vivo* tumors and further confirm the efficacy of YM-155, we developed 3D-spheroid models using cells from two human NB cell lines, one MYCN Non-amplified- SH-SY5Y and one MYCN Amplified- IMR-32. These 3D models generate a solid anchorage-independent cell spheroid mass that closely mimics the *in vivo* growth of solid NB tumors. As shown in **Figure 13** for SH-SY5Y and in **Figure 14** for IMR-32, similar size spheroids were developed, randomized, and subjected to increasing doses of YM-155 (day 0). The size of each spheroid was measured and imaged on day 0, 3, 6, 9 and 12 (**Figure 13A -SH-SY5Y and 14A -IMR-32**). Results showed a significant, dose-dependent inhibition of spheroid growth by YM-155 in comparison to control treatment (**Figure 13B -SH-SY5Y and 14B -IMR-32**).

Furthermore, Calcein AM and EthD-III staining, and live cell ATP releasing assay performed on the spheroids demonstrated that YM-155 treatment significantly, and in a dose-dependent manner induces tumor cell death to inhibit spheroid growth in SH-SY-5Y (**Figure 15**), and IMR-32 (**Figure 16**). Calcein AM dye stains live cells and yields green fluorescence, whereas EthD-III dye stains dead cells and yields red fluorescence. Overall, these results recognized the potency of YM-155 on NB spheroid tumor growth.

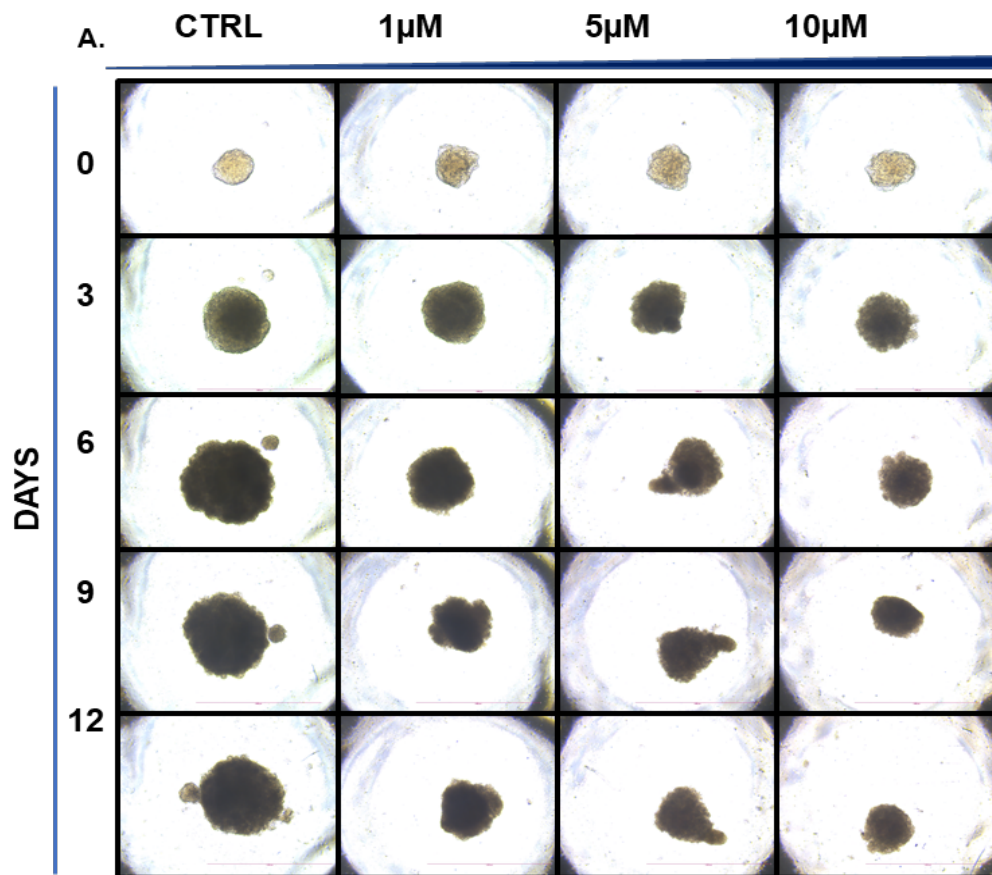


**Figure 13 (A): YM-155 inhibits NB spheroid tumor growth in SH-SY5Y cells.** Representative spheroid images every three days for 12 days in response to YM-155 treatment.

B.

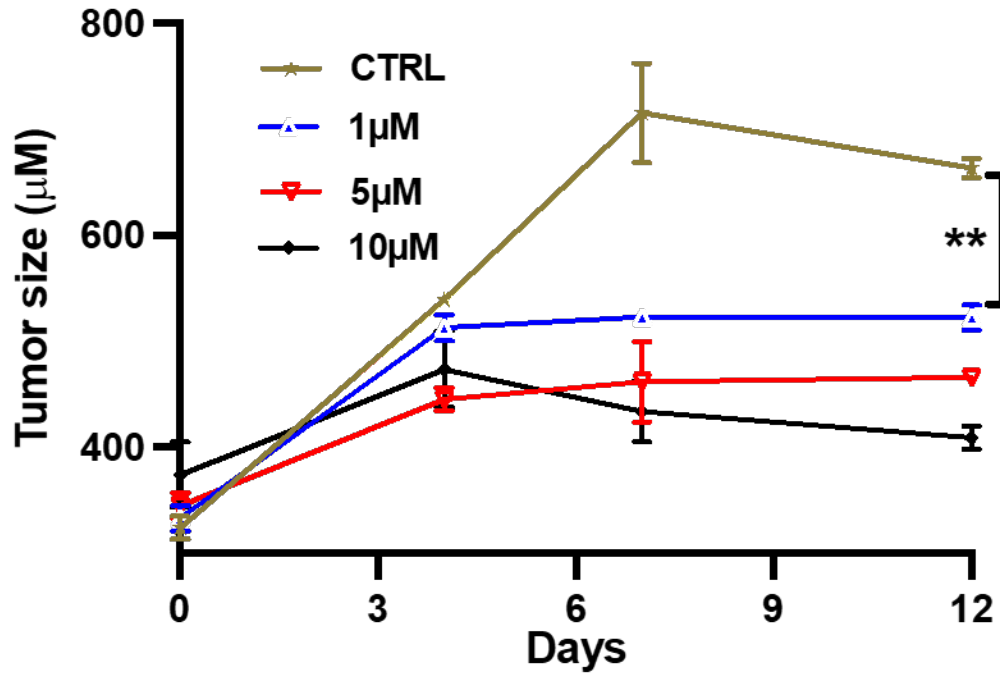
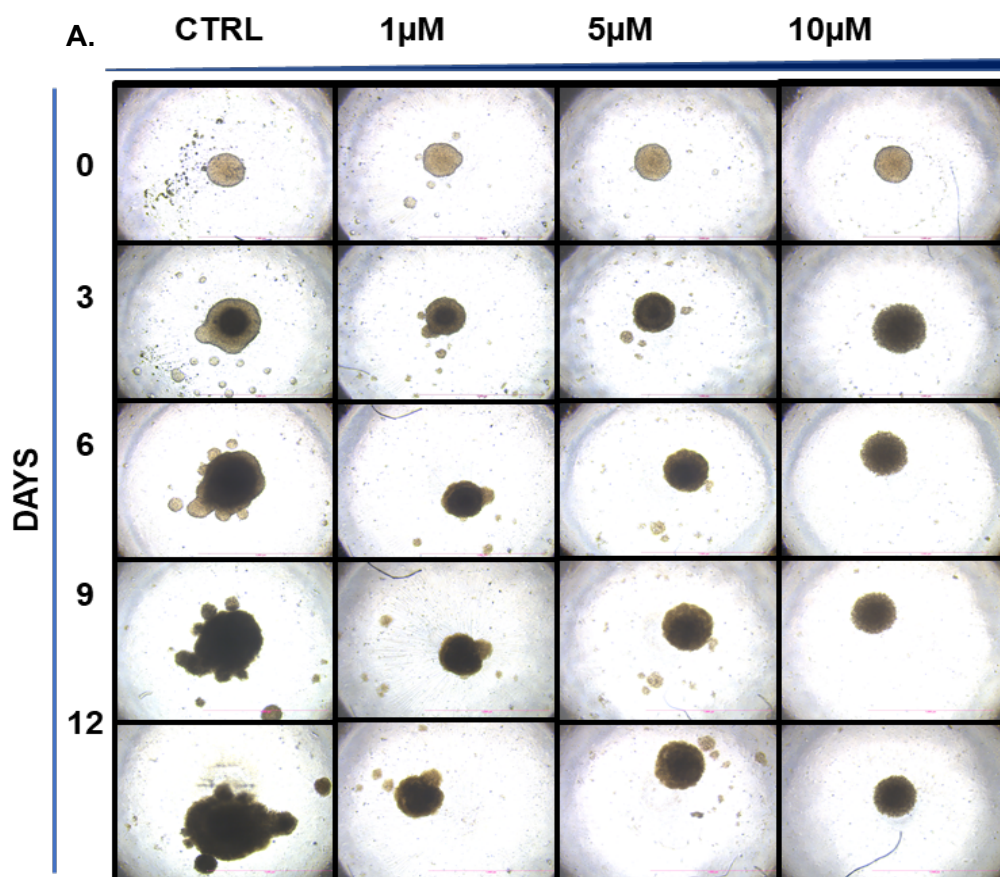


Figure 13 (B): YM-155 inhibits NB spheroid tumor growth in SH-SY5Y cells.

Quantitative representation of spheroid tumor growth size as displayed in **Figure 13A**.

\*\* p<0.01



**Figure 14 (A): YM-155 inhibits NB spheroid tumor growth in IMR-32 cells.** Representative spheroid images every three days for 12 days in response to YM-155 treatment.

B.

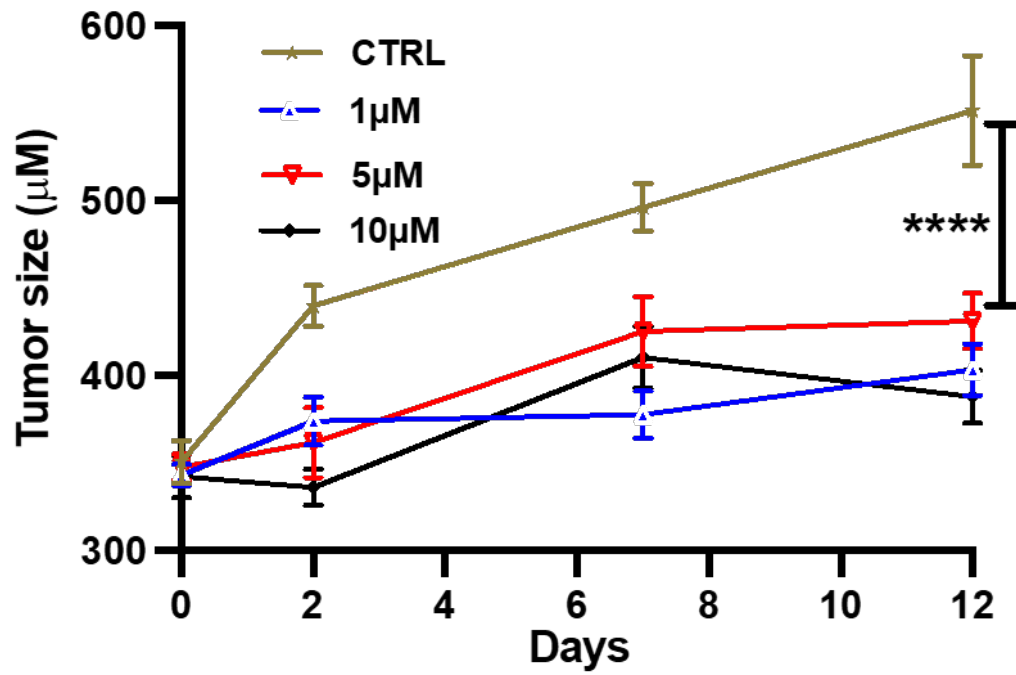
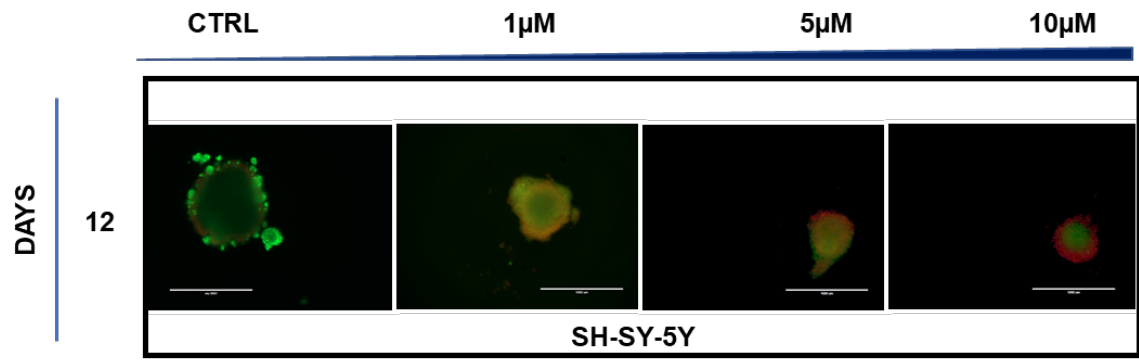


Figure 14 (B): YM-155 inhibits NB spheroid tumor growth in IMR-32 cells.

Quantitative representation of spheroid tumor growth size as displayed in **Figure 14 A**.

\*\*\*\*  $p < 0.0001$

A.



**Figure 15 (A.): YM-155 inhibits NB 3D-spheroid tumor growth in SH-SY5Y cells.** Representative spheroid images of terminal spheroids on day 12 stained with Calcein AM and EthD-III fluorescence dyes, in response to YM-155 treatment in SH-SY5Y cells. Quantitative representation of the percentage of cells stained with Calcein AM and EthD-III on day 12 in SH-SY5Y cells.

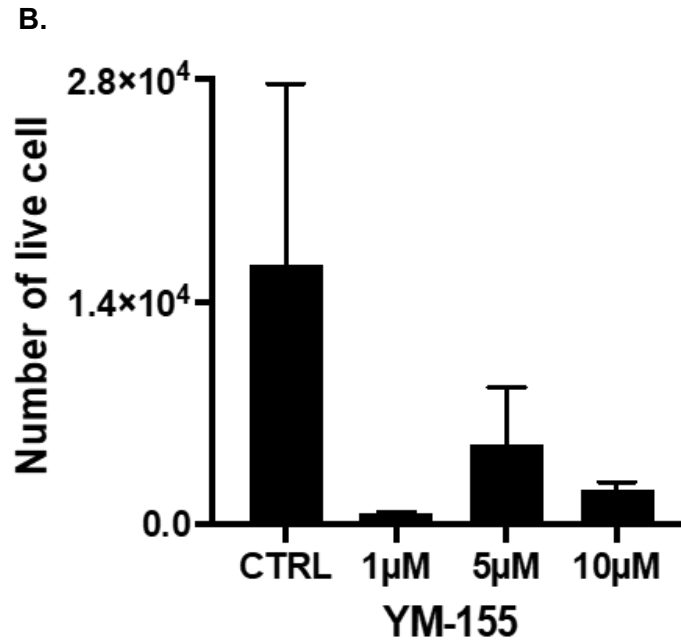


**Figure 15 (B): YM-155 inhibits NB 3D-spheroid tumor growth in SH-SY5Y cells.**

ATP releasing assay quantitative measurement of number of live cells in terminal spheroids on day 12 in SH-SY5Y cells.

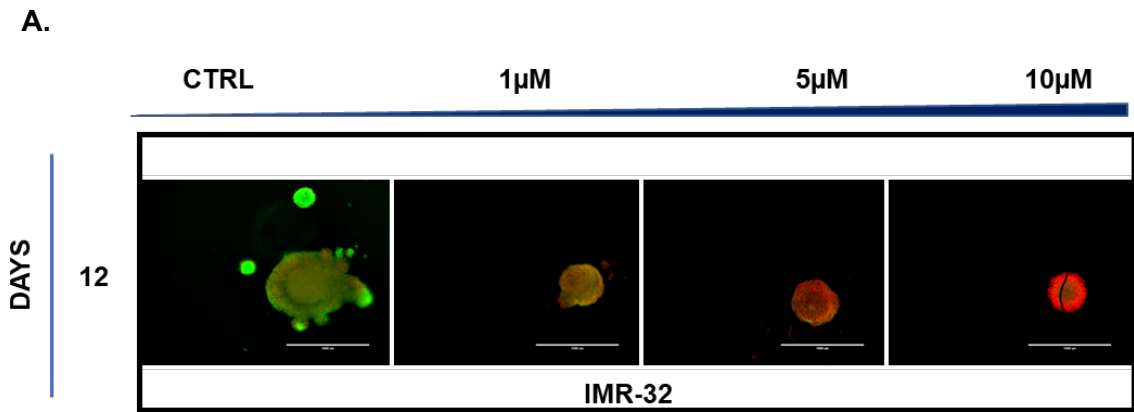


**Figure 16 (A): YM-155 inhibits NB 3D-spheroid tumor growth in IMR-32 cells.** Representative spheroid images of terminal spheroids on day 12 stained with Calcein AM and EthD-III fluorescence dyes, in response to YM-155 treatment in IMR-32 cells. Quantitative representation of the percentage of cells stained with Calcein AM and EthD-III on day 12 in IMR-32 cells .

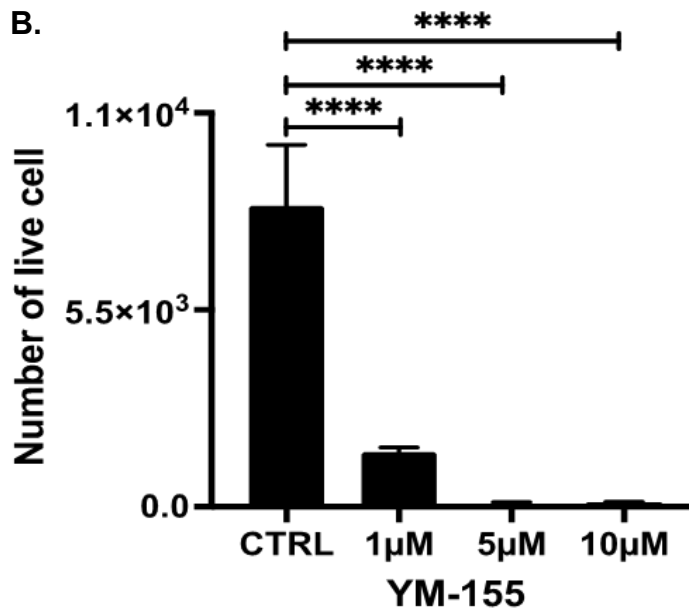


**Figure 16 (B): YM-155 inhibits NB 3D-spheroid tumor growth in IMR-32 cells.**  
ATP releasing assay quantitative measurement of number of live cells in terminal spheroids on day 12 in IMR-32 cells. \*\*\*\* p<0.0001

### **3.5 YM-155 INHIBITS SURVIVIN PATHWAY TO SUPPRESS NB GROWTH**

YM-155 is known to directly inhibit survivin which in turn inhibits the overall survivin pathway. Therefore, we performed RT-qPCR assays and Western blot assays to further explicate the mechanism of action of YM-155 in NB. RT-qPCR assay results showed that YM-155 significantly inhibits the mRNA expression of BIRC5, TP53, BCL2, NOXA, and PUMA genes in a dose-dependent manner as compared to the controls (**Figure 17**).

Additionally, Western blot assays showed that YM-155 inhibits survivin protein levels as well as p53 (**Figure 18A**) in comparison to control. Additionally, Western blot assays were also performed for testing a combination of YM-155 and RG-7388 and results showed a sensitization of NB to YM-155 in the presence of RG-7388 and an increase in p53 protein expression (**Figure 18B**). Overall, our molecular assays showed that YM-155 inhibits survivin at both the mRNA and protein levels, thereby leading to the inhibition of the oncogenic survivin pathway in NB.

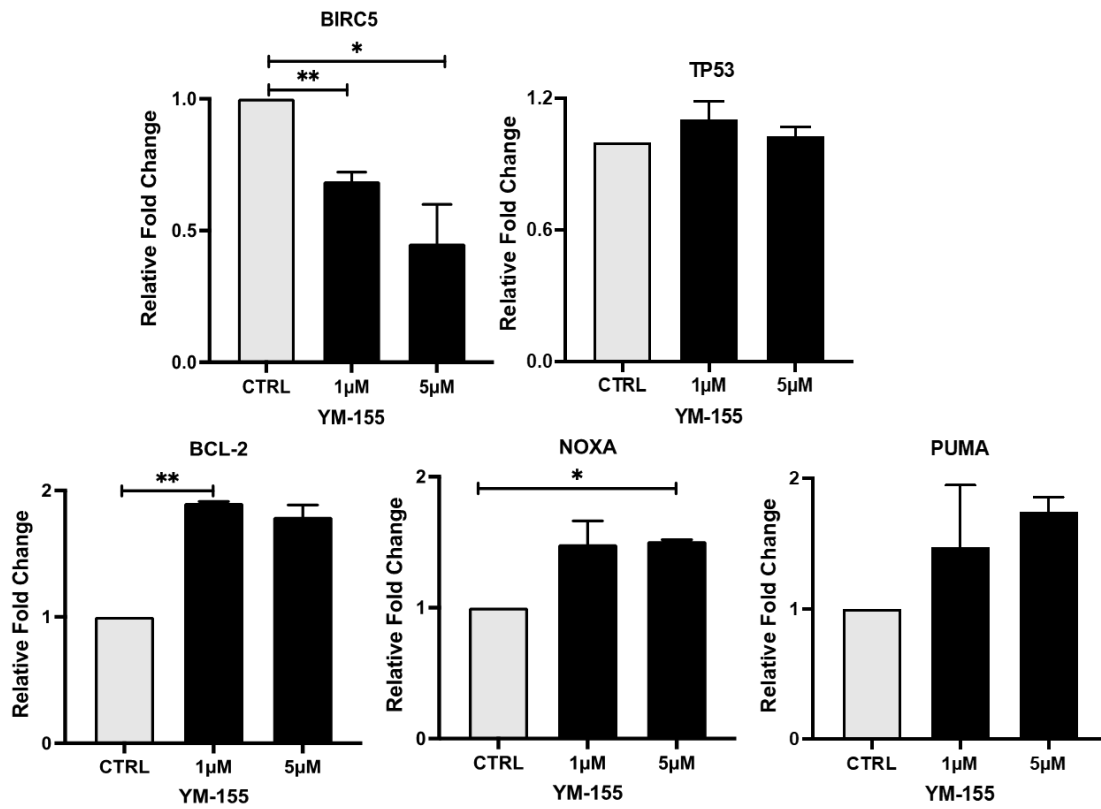


**Figure 17: YM-155 inhibits Survivin pathway at mRNA level.** Gene expression analysis of BIRC5, TP53, BCL-2, NOXA, and PUMA in response to YM-155 treatments in SH-SY5Y cells. \*  $p < 0.05$ ; \*\*  $p < 0.01$

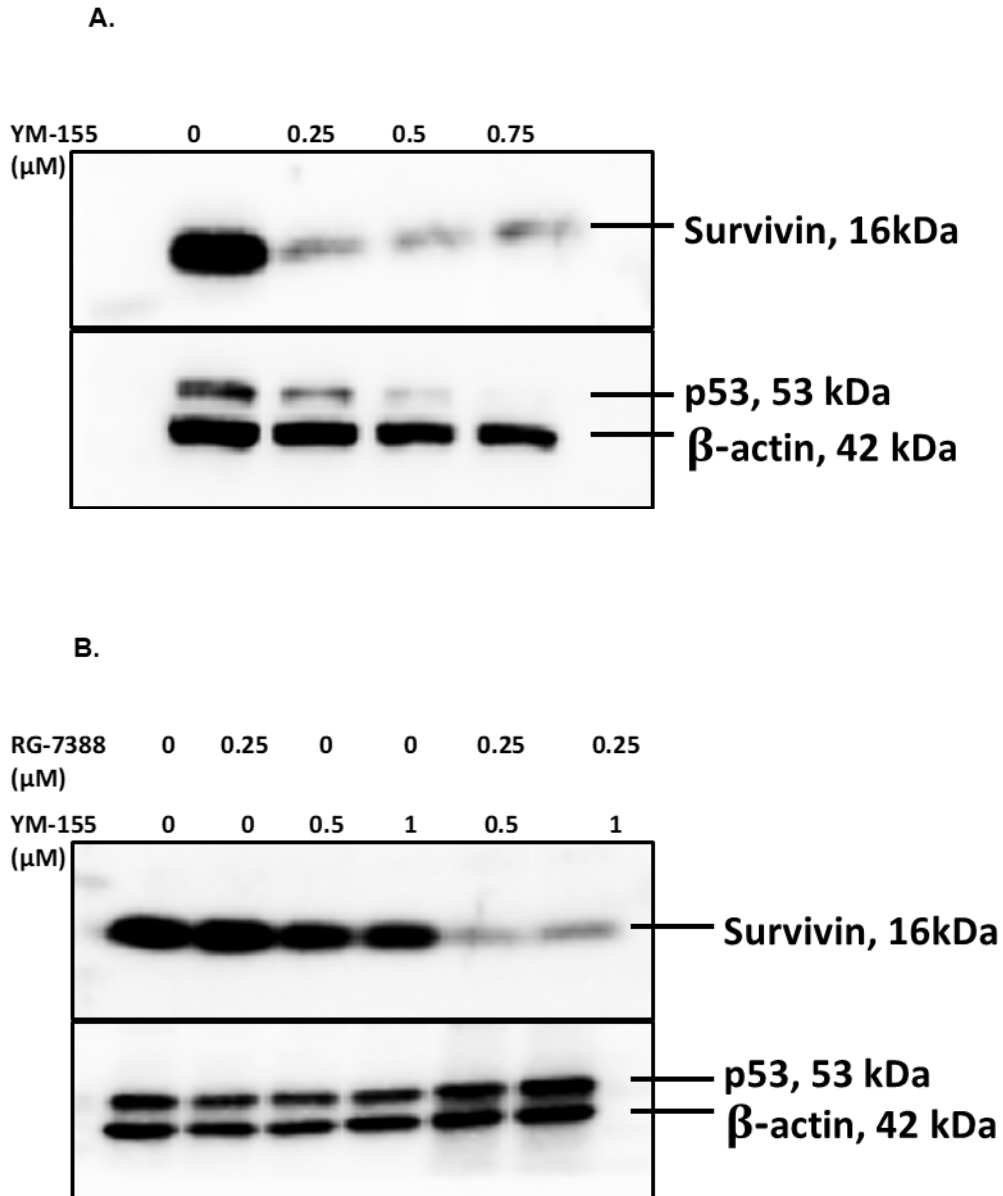


**Figure 18: YM-155 inhibits Survivin pathway at protein level. (A and B)** Western blot analysis of various apoptotic pathway proteins in response to increasing concentrations of YM-155 treatments in NGP cells for 24 hours.  $\beta$ -actin was used as loading control.

### **3.6 YM-155 SENSITIZES NB TO CHEMOTHERAPY**

VP-16 is one of the most active chemotherapeutic drugs for other cancers, such as refractory pediatric neoplasms, hepatocellular carcinomas, acute nonlymphocytic leukemia, prostatic carcinomas, ovarian carcinomas, and non-small cell lung cancer (Reyhanoglu and Tadi, 2021). Therefore, we evaluated VP-16 and YM-155 combination therapy for treating NB and observed whether YM-155 sensitizes NB to VP-16. We utilized 6 NB cell lines including 3 MYCN Non-amplified (SH-SY5Y, SK-N-AS, CHLA-255) and 3 MYCN Amplified (NGP, LAN5, IMR-32), and cell proliferation assays were performed by treating the cells with either drug alone or with combination ratios, then analyzed using GraphPad PRISM 8 and CompuSyn (Chou-Talalay method) software as shown in **(Figure 19 and 20)**.

Results showed that YM-155 and VP-16 act synergistically to significantly inhibit NB cell proliferation in comparison to either drug alone **(Figure 19A and 20A)**. The combination indexes (CIs) were determined for MYCN Non-amplified **(Figure 21)** and MYCN Amplified **(Figure 22)**. The effective dose (ED); ED<sub>50</sub>, ED<sub>75</sub>, ED<sub>90</sub>, and ED<sub>95</sub> were observed to be lower than 1.0 in most cases, indicating a synergistic effect between YM-155 and VP-16 in NB, some exceptions applied where antagonistic effects were observed (CI >1): at ED<sub>50</sub> (SH-SY5Y & CHLA-255); at ED<sub>50</sub> and ED<sub>75</sub> (NGP & IMR-32), and at ED<sub>95</sub> LAN-5. Overall, our results indicated that inhibiting survivin pathway by using YM-155 and combining it with a known chemotherapeutic is a novel therapeutic approach for NB treatment.

A.

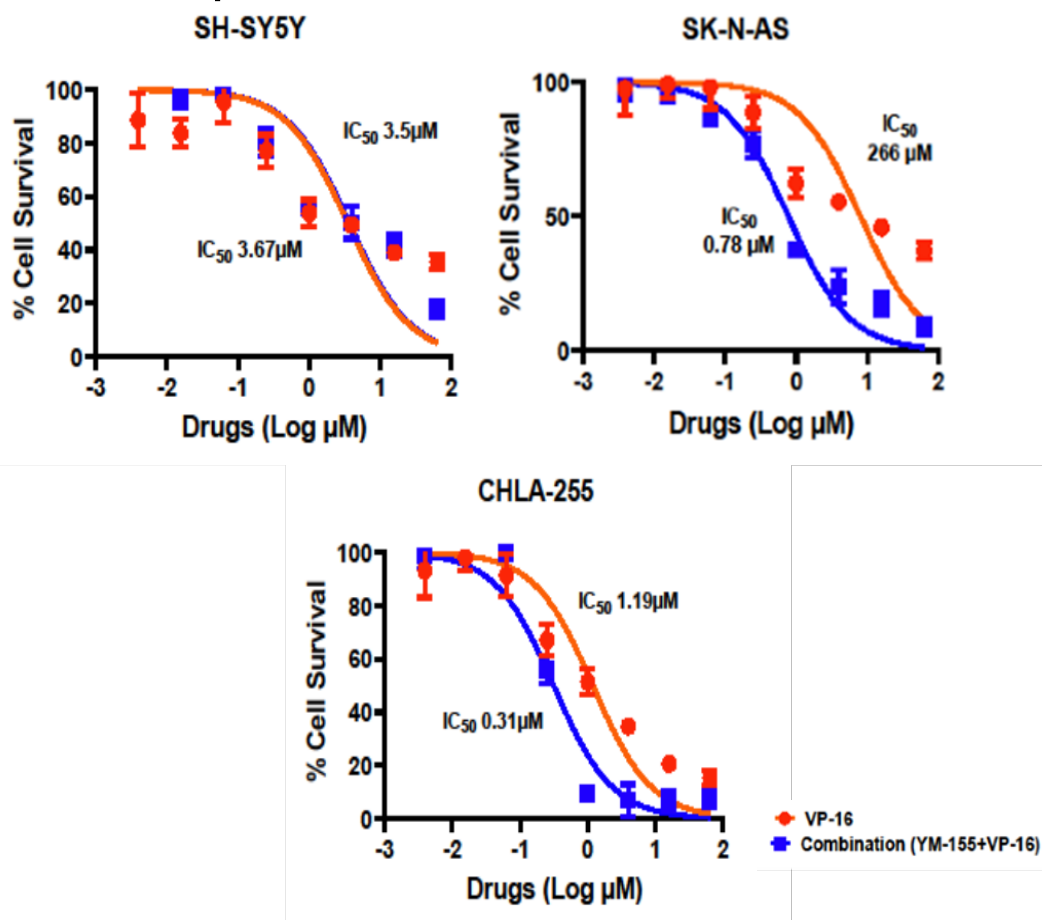


**Figure 19 (A): YM-155 enhances VP-16 induced cytotoxicity in MYCN Non-amplified NB cell lines.** Cytotoxicity of YM-155 in combination with VP-16 was measured by using MTT dye for NB cell lines with treatment ratio of 0.004:1 (VP-16:YM-155) in MYCN Non-amplified cell lines. SH-SY5Y, SK-N-AS, CHLA-255, were treated with different combinations at 72-hour time points, then MTT assay was performed. The absorbance of each well was measured and plotted as a cell viability curve. Results were analyzed using GraphPad PRISM 8 software. Synergistic effect was observed.

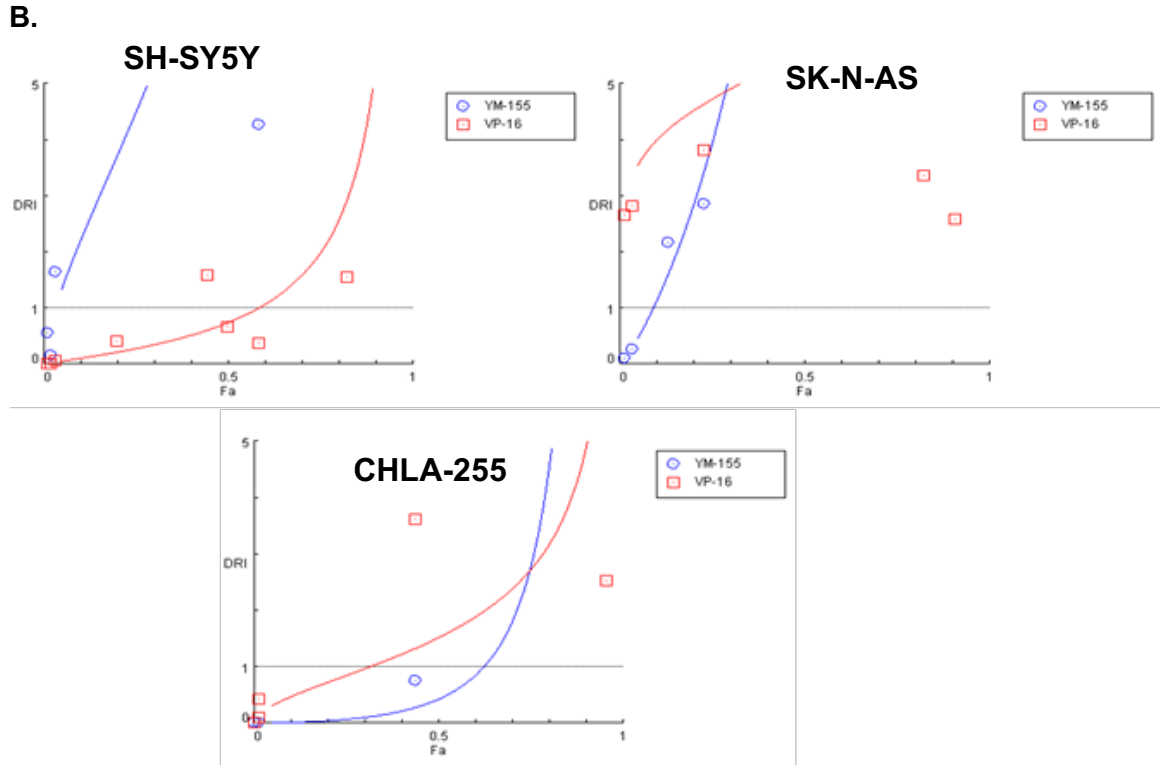


**Figure 19 (B): YM-155 enhances VP-16 induced cytotoxicity in MYCN Non-amplified NB cell lines.** Dose response index (DRI) graphs were plotted using CompuSyn software and Chou-Talalay CI method. DRI plots for MYCN Non-amplified cell lines showed synergistic effect of drug combination.

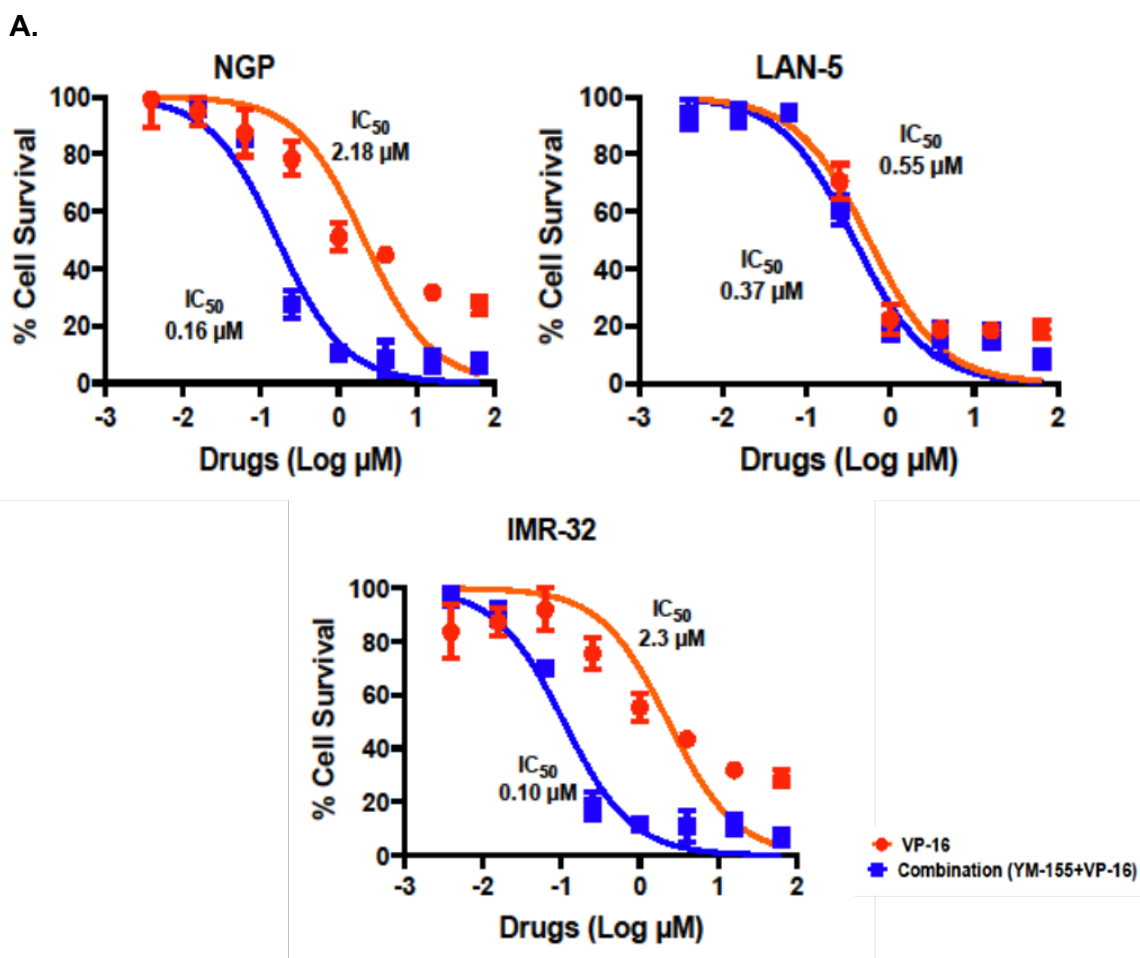


**Figure 20 (A): YM-155 enhances VP-16 induced cytotoxicity in MYCN Amplified NB cell lines.** Cytotoxicity of YM-155 in combination with VP-16 was measured by using MTT dye for NB cell lines with treatment ratio of 0.125:1(VP-16:YM-155) in MYCN Amplified cell lines. NGP, LAN-5, and IMR-32 were treated with different combinations at 72-hour time point, then MTT assay was performed. The absorbance of each well was measured and plotted as a cell viability curve. Results were analyzed using GraphPad PRISM 8 software. Synergistic effect was observed.

**B.**

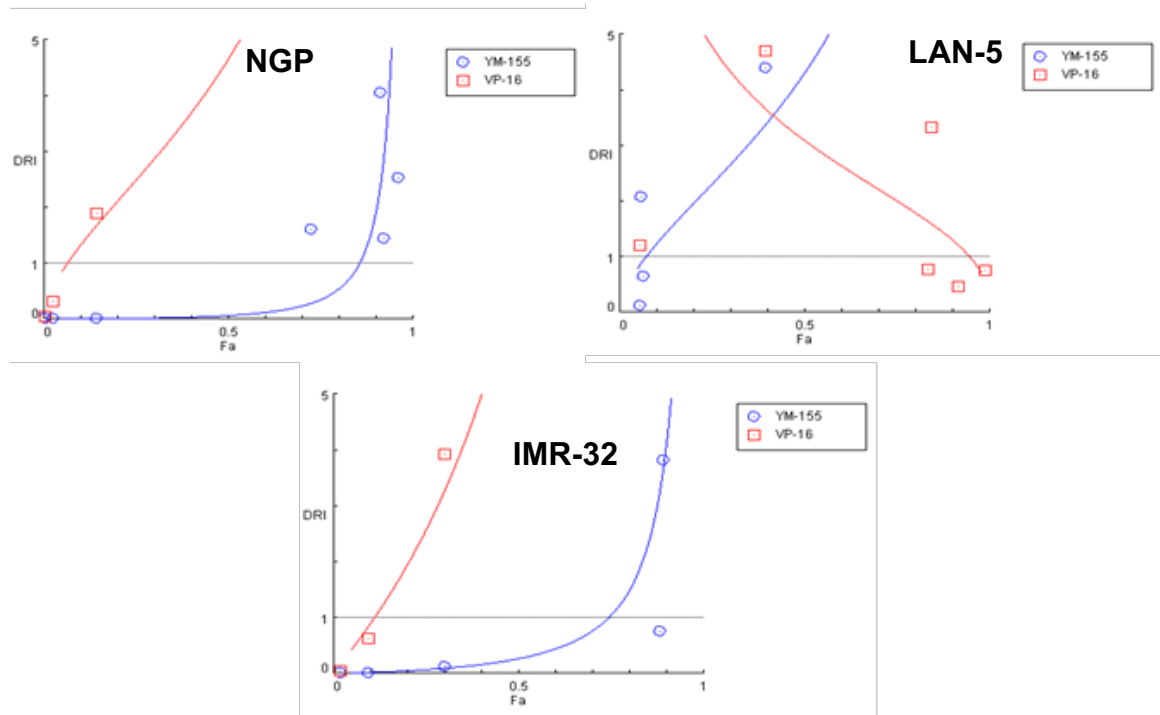


**Figure 20 (B): YM-155 enhances VP-16 induced cytotoxicity in MYCN Amplified NB cell lines.** Dose response index (DRI) graphs were plotted using CompuSyn software and Chou-Talalay CI method. DRI plots for MYCN Amplified cell lines showed synergistic effect of drug combination.

A.

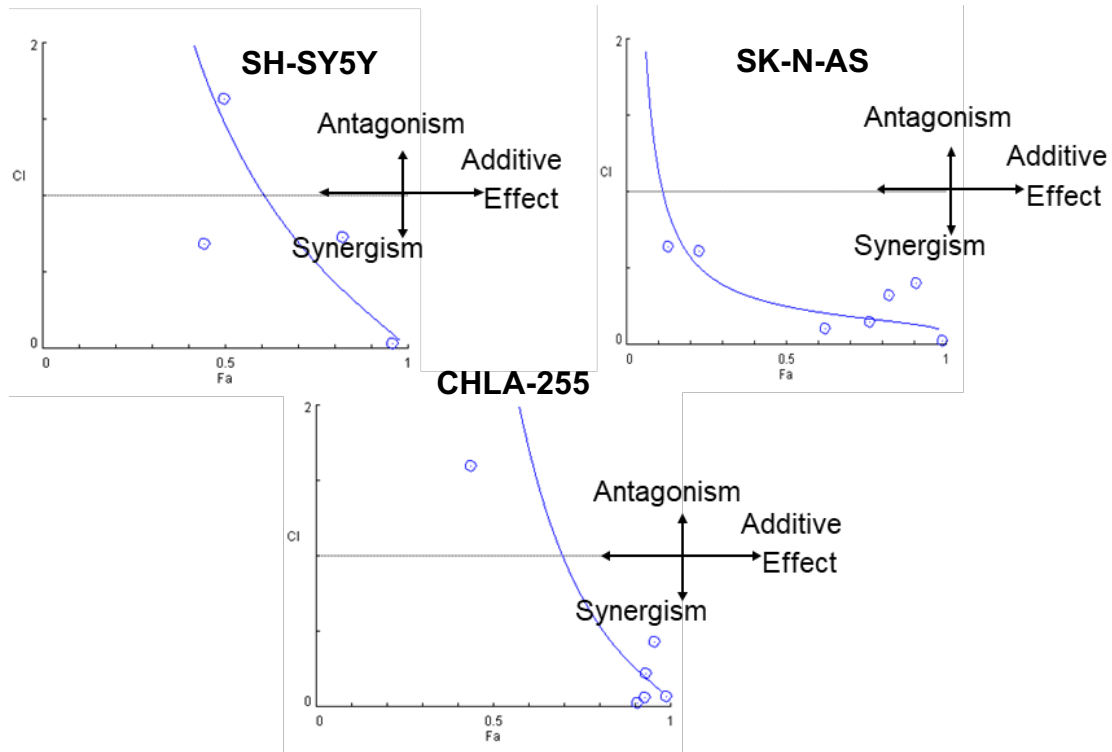


**Figure 21 (A): YM-155 sensitizes NB MYCN Non-amplified cell lines to chemotherapy VP-16.** CI studies were performed by cell cytotoxicity assays in response to either VP-16 alone or in combination with YM-155 in NB cell lines at a ratio of 0.004:1(VP-16:YM-155) in MYCN Non-amplified: SH-SY5Y, SK-N-AS, CHLA-255. Shown is the representative CI Plot. Values of  $CI < 1$ ,  $= 1$  and  $> 1$  indicate synergism, additive effects and antagonism, respectively.

**B.**

<b>Combinational Index (CI)</b>				
<b>Cell line</b>	<b>ED50</b>	<b>ED75</b>	<b>ED90</b>	<b>ED95</b>
<b>SH-SY5Y</b>	<b>1.46220</b>	<b>0.55693</b>	<b>0.21359</b>	<b>0.11183</b>
<b>SK-N-AS</b>	<b>0.25173</b>	<b>0.17226</b>	<b>0.13403</b>	<b>0.11681</b>
<b>CHLA-255</b>	<b>3.01911</b>	<b>0.72605</b>	<b>0.25878</b>	<b>0.15218</b>

*\* Note: CI<1 indicates synergism; C=1 indicates additive effect; C>1 indicates antagonism*

**Figure 21 (B): YM-155 sensitizes NB MYCN Non-amplified cell lines to chemotherapy VP-16.** CI studies were performed by cell cytotoxicity assays in response to either VP-16 alone or in combination with YM-155 in NB cell lines at a ratio of 0.004:1(VP-16:YM-155) in MYCN Non-amplified: SH-SY5Y, SK-N-AS, CHLA-255. Summary of drug synergy values represented as CI. CI values for the combination of YM-155 and VP-16 at different effective doses (ED<sub>50</sub>, ED<sub>75</sub>, ED<sub>90</sub>, ED<sub>95</sub>). CI values were calculated by the Chou-Talalay method for drug interactions using CompuSyn software for the different fractions affected. Values of CI < 1, = 1 and >1 indicate synergism, additive effects and antagonism, respectively.

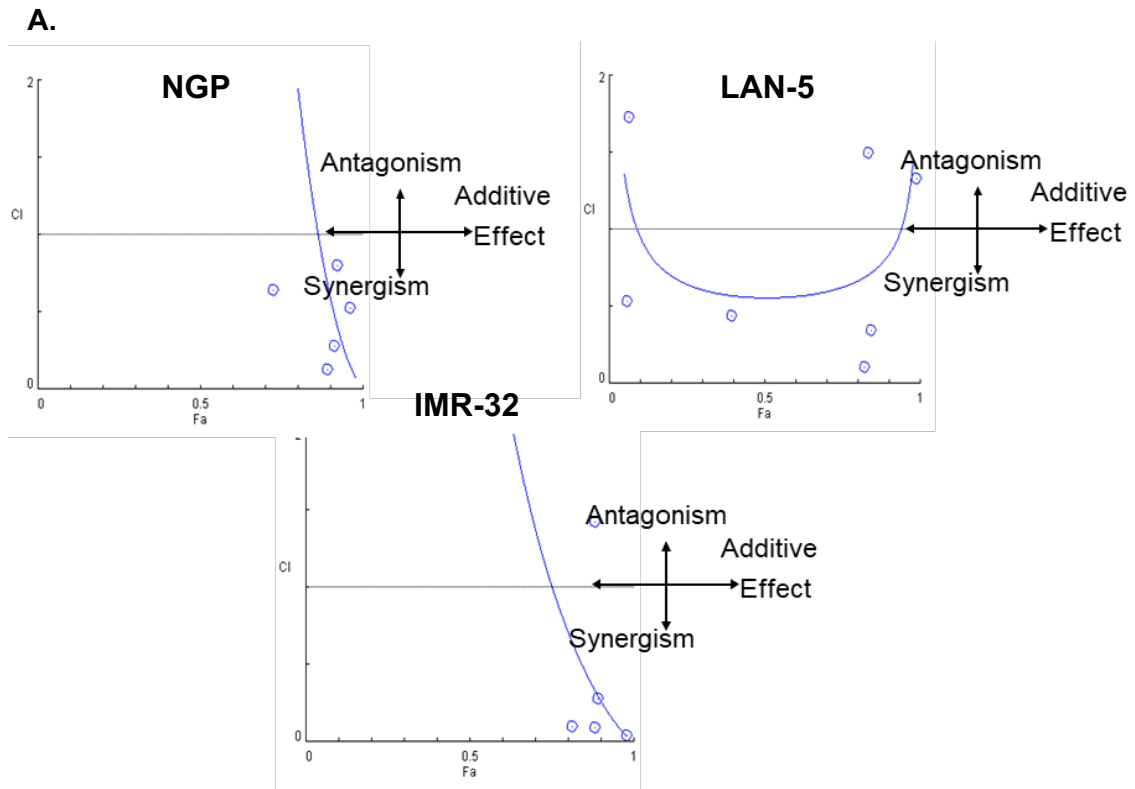


**Figure 22 (A): YM-155 sensitizes NB MYCN Amplified cell lines to chemotherapy VP-16.** CI studies were performed by cell cytotoxicity assays in response to either VP-16 alone or in combination with YM-155 in NB cell lines at a ratio of 0.125:1 (VP-16:YM-155) in MYCN Amplified cell lines: NGP, LAN-5, and IMR-32. Shown is the CI Plot. Values of  $CI < 1$ ,  $= 1$  and  $> 1$  indicate synergism, additive effects, and antagonism, respectively.

**B.**

<b>Combinational Index (CI)</b>				
<b>Cell line</b>	<b>ED50</b>	<b>ED75</b>	<b>ED90</b>	<b>ED95</b>
<b>NGP</b>	<b>16.1612</b>	<b>3.00495</b>	<b>0.58516</b>	<b>0.20400</b>
<b>LAN-5</b>	<b>0.55617</b>	<b>0.62475</b>	<b>0.83931</b>	<b>1.08192</b>
<b>IMR-32</b>	<b>3.91575</b>	<b>1.00576</b>	<b>0.25957</b>	<b>0.10368</b>

*\* Note: CI<1 indicates synergism; C=1 indicates additive effect; C>1 indicates antagonism*

**Figure 22 (B): YM-155 sensitizes NB MYCN Amplified cell lines to chemotherapy VP-16.** CI studies were performed by cell cytotoxicity assays in response to either VP-16 alone or in combination with YM-155 in NB cell lines at a ratio of 0.125:1 (VP-16:YM-155) in MYCN Amplified cell lines: NGP, LAN-5, and IMR-32. Summary of drug synergy values represented as CI. CI values for the combination of YM-155 and VP-16 at different effective doses (ED<sub>50</sub>, ED<sub>75</sub>, ED<sub>90</sub>, ED<sub>95</sub>). CI values were calculated by the Chou-Talalay method for drug interactions using CompuSyn software for the different fractions affected. Values of CI < 1, = 1 and > 1 indicate synergism, additive effects and antagonism, respectively.

## CHAPTER 4

### 4. DISCUSSION

For a tumor to become established, compromises in the control of cell proliferation as well as in the control of cell death are necessary (Lu *et al.*, 1998). This simple yet profound statement is still applicable and relevant in today's NB cancer research, as we seek to discover the mechanism of action driving proliferation and thereby create targeted, novel, less toxic and more efficacious treatments for those suffering from this deadly disease. It is known that the main clinical interest in survivin is undoubtedly in cancer, ranking fourth in the most upregulated mRNA in the human cancer transcriptome and its expression has been correlated with increased tumor resistance to a broad range of chemotherapy agents, radiation insensitivity and poor patient prognosis (Wheatley and Altieri, 2019). In literature, the imbalance of its natural cycle of expression has been due principally to transcriptional de-repression, which causes continuous synthesis throughout the cell and altered splicing. Hence, it is clear that with roles in mitosis, apoptosis suppression, autophagy, migration, metabolism and angiogenesis, there are many routes through which survivin can promote tumor cell survival and cancer metastasis (Wheatley and Altieri, 2019).

In our study we sought to explore how YM-155, a direct survivin inhibitor alone and then in combination with VP-16, one of the most commonly used topoisomerase (an enzyme required for DNA synthesis and topology alteration) inhibitor, would affect NB proliferation (Xian *et al.*, 2007). The anticancer mechanistic action of YM-155 has been under dispute and may depend on the cellular background. YM-155 was introduced as a

compound that suppresses the expression of survivin. However, other studies suggested that YM-155 may primarily induce DNA damage and that the reduction of survivin levels may rather be a consequence of DNA damage (Voges *et al.*, 2016). In our study, this was confirmed by cell cycle analysis where the cell cycle S phase (synthesis phase: DNA Replication) was inhibited, which blocked cell cycle progression in the G0/G1 phase. Gene expression analysis of NB tumors from patients revealed that reduced survivin strongly correlates with increased overall survival and reduced disease progression of NB. The gene expression analysis of NB tumors from patients also revealed that survivin strongly correlates with MYCN amplification and expression. Additionally using RG-7388, NB was made more susceptible to treatment, as observed in literature. RG-7388 has a potent apoptotic effect on NB cells, which is dependent on the presence of wild-type p53 (Lakoma *et al.*, 2015).

In the present study, for the first time to the best of our knowledge, we reported that YM-155 blocks cell cycle advancement in the S-phase, and thereby prevents oncogenic progression of NB. Therefore, our results established that survivin inhibition is a promising therapeutic strategy for NB. Through the inhibition of survivin, YM-155 inhibits protein synthesis on the molecular level, decreases gene expression in anti-apoptotic genes, induces apoptosis in a dose-dependent manner in NB cells by increasing expression of apoptotic genes and its subsequent signaling pathway that controls different tumor suppressor genes, such as, BCL-2, PUMA, and NOXA. We also concluded that YM-155 inhibits the NB cell proliferation and induces apoptosis by inducing cell cycle synthesis (S) phase arrest. Our *in vitro* 3D tumor studies showed dose-dependent tumor size reduction. Previous studies on anticancer effects of both Am-ZnO NPs and DOX-HCl on

A549 tumor spheroids reported that the 3D tumor model (spheroids) is the best *ex vivo* model for the anticancer drug screening because their structure mimics the tumor microenvironment of a solid cancer. Such screening has reduced the *in vivo* testing of anticancer drugs (Chabattula *et al.*, 2021). We also utilized the widely used 3D spheroidal assays model system to determine drug effects in cancer. We have developed a dual combination therapy approach by combining YM-155 with VP-16 to develop a less-toxic and more efficacious therapeutic approach for the treatment of NB. Our results demonstrated that YM-155 and VP-16 are synergistic and inhibits NB growth in both 2D proliferation assays and 3D spheroid model.

Conclusively, our data shows that YM-155 affects the viability of NB cells, including NB cells with acquired resistance to clinically relevant drugs through survivin depletion, and that survivin is a promising drug target in NB cells with acquired drug resistance. YM-155 significantly inhibits NB cell proliferation, colony growth, blocks cell cycle progression, induce apoptosis, and inhibit 3D spheroid tumor formation and growth in a dose-dependent manner. Dual therapeutic approach of combining YM-155 and VP-16 could be a potential therapeutic strategy for treating high-risk therapy-resistant or refractory NB patients. In future efforts we hope to further explore the *in vivo* potency of YM-155 alone and in combination with known chemotherapeutics using NB mice models.

## REFERENCES

1. Agarwal S, Ghosh R, Chen Z, Lakoma A, Gunaratne PH, Kim ES, and Shohet JM (2016) Transmembrane adaptor protein PAG1 is a novel tumor suppressor in neuroblastoma. *Oncotarget* **7**:24018–24026.
2. Agarwal S, Lakoma A, Chen Z, Hicks J, Metelitsa LS, Kim ES, and Shohet JM (2015) G-CSF Promotes Neuroblastoma Tumorigenicity and Metastasis via STAT3-Dependent Cancer Stem Cell Activation. *Cancer Res* **75**:2566–2579, American Association for Cancer Research.
3. Agarwal S, Milazzo G, Rajapakshe K, Bernardi R, Chen Z, Barberi E, Koster J, Perini G, Coarfa C, and Shohet JM (2018) MYCN acts as a direct co-regulator of p53 in MYCN amplified neuroblastoma. *Oncotarget* **9**:20323–20338.
4. Chabattula SC, Gupta PK, Tripathi SK, Gahtori R, Padhi P, Mahapatra S, Biswal BK, Singh SK, Dua K, Ruokolainen J, Mishra YK, Jha NK, Bishi DK, and Kesari KK (2021) Anticancer therapeutic efficacy of biogenic Am-ZnO nanoparticles on 2D and 3D tumor models. *Mater Today Chem* **22**:100618.
5. Cheng SM, Lin T-Y, Chang Y-C, Lin I-W, Leung E, and Cheung CHA (2021) YM155 and BIRC5 downregulation induce genomic instability via autophagy-mediated ROS production and inhibition in DNA repair. *Pharmacol Res* **166**:105474.
6. Cheung CHA, Huang C-C, Tsai F-Y, Lee JY-C, Cheng SM, Chang Y-C, Huang Y-C, Chen S-H, and Chang J-Y (2013) Survivin &ndash; biology and potential as a therapeutic target in oncology. *OncoTargets Ther* **6**:1453–1462, Dove Press.
7. Efeyan A, and Serrano M (2007) p53: Guardian of the Genome and Policeman of the Oncogenes. *Cell Cycle* **6**:1006–1010, Taylor & Francis.
8. Fetahu IS, and Taschner-Mandl S (2021) Neuroblastoma and the epigenome. *Cancer Metastasis Rev* **40**:173–189.
9. Frassanito MA, Saltarella I, Vinella A, Muzio LL, Pannone G, Fumarulo R, Vacca A, and Marigliò MA (2019) Survivin overexpression in head and neck squamous cell carcinomas as a new therapeutic target (Review). *Oncol Rep* **41**:2615–2624, Spandidos Publications.
10. Guan S, Lu J, Zhao Y, Yu Y, Li H, Chen Z, Shi Z, Liang H, Wang M, Guo K, Chen X, Sun W, Bieerkehazhi S, Xu X, Sun S, Agarwal S, and Yang J (2017) MELK is a novel therapeutic target in high-risk neuroblastoma. *Oncotarget* **9**:2591–2602.

11. Huang M, and Weiss WA (2013) Neuroblastoma and MYCN. *Cold Spring Harb Perspect Med* **3**:a014415, Cold Spring Harbor Laboratory Press.
12. Kudchadkar R, Ernst S, Chmielowski B, Redman BG, Steinberg J, Keating A, Jie F, Chen C, Gonzalez R, and Weber J (2015) A phase 2, multicenter, open-label study of sepantronium bromide (YM155) plus docetaxel in patients with stage III (unresectable) or stage IV melanoma. *Cancer Med* **4**:643–650.
13. Lakoma A, Barbieri E, Agarwal S, Jackson J, Chen Z, Kim Y, McVay M, Shoheit JM, and Kim ES (2015) The MDM2 small-molecule inhibitor RG7388 leads to potent tumor inhibition in p53 wild-type neuroblastoma. *Cell Death Discov* **1**:1–9.
14. Lu C-D, Altieri DC, and Tanigawa N (1998) Expression of A Novel Antiapoptosis Gene, Survivin, Correlated with Tumor Cell Apoptosis and p53 Accumulation in Gastric Carcinomas. *Cancer Res* **58**:1808–1812, American Association for Cancer Research.
15. Maris JM (2010) Recent Advances in Neuroblastoma. *N Engl J Med* **362**:2202–2211, Massachusetts Medical Society.
16. Rauch A, Hennig D, Schäfer C, Wirth M, Marx C, Heinzl T, Schneider G, and Krämer OH (2014) Survivin and YM155: How faithful is the liaison? *Biochim Biophys Acta BBA - Rev Cancer* **1845**:202–220.
17. Smith V, and Foster J (2018) High-Risk Neuroblastoma Treatment Review. *Children* **5**:114, Multidisciplinary Digital Publishing Institute.
18. Sun W, Rojas Y, Wang H, Yu Y, Wang Y, Chen Z, Rajapakshe K, Xu X, Huang W, Agarwal S, Patel RH, Woodfield S, Zhao Y, Jin J, Zhang H, Major A, Hicks MJ, Shoheit JM, Vasudevan SA, Coarfa C, Yang J, and Nuchtern JG (2017) EWS-FLI1 and RNA helicase A interaction inhibitor YK-4-279 inhibits growth of neuroblastoma. *Oncotarget* **8**:94780–94792.
19. Tweddle DA, Pearson ADJ, Haber M, Norris MD, Xue C, Flemming C, and Lunec J (2003) The p53 pathway and its inactivation in neuroblastoma. *Cancer Lett* **197**:93–98.
20. Voges Y, Michaelis M, Rothweiler F, Schaller T, Schneider C, Politt K, Mernberger M, Nist A, Stiewe T, Wass MN, Rödel F, and Cinatl J (2016) Effects of YM155 on survivin levels and viability in neuroblastoma cells with acquired drug resistance. *Cell Death Dis* **7**:e2410–e2410.
21. Wheatley SP, and Altieri DC (2019) Survivin at a glance. *J Cell Sci* **132**:jcs223826.

22. Xian CJ, Cool JC, van Gangelen J, Foster BK, and Howarth GS (2007) Effects of etoposide and cyclophosphamide acute chemotherapy on growth plate and metaphyseal bone in rats. *Cancer Biol Ther* **6**:170–177, Taylor & Francis.
23. Yi JS, Sias-Garcia O, Nasholm N, Hu X, Iniguez AB, Hall MD, Davis M, Guha R, Moreno-Smith M, Barbieri E, Duong K, Koach J, Qi J, Bradner JE, Stegmaier K, Weiss WA, and Gustafson WC (2021) The synergy of BET inhibitors with aurora A kinase inhibitors in MYCN-amplified neuroblastoma is heightened with functional TP53. *Neoplasia* **23**:624–633.

Vita

Name	<i>Danielle C. Rouse</i>
Baccalaureate Degree	<i>Bachelor of Science John Jay College of Criminal Justice (CUNY), New York Major: Forensic Science conc. Toxicology</i>
Date Graduated	<i>June, 2016</i>
Associate Degree	<i>Associate of Science Barbados Community College, Barbados, Major: Biology, Chemistry, Mathematics</i>
Date Graduated	<i>July, 2012</i>